Brain, Behavior, & Immunity - Health 43 (2025) 100908

Contents lists available at ScienceDirect

Brain, Behavior, & Immunity - Health

journal homepage: www.editorialmanager.com/bbih/default.aspx

Repeated social defeat in male mice induced unique RNA profiles in projection neurons from the amygdala to the hippocampus

Rebecca G. Biltz [a], Wenyuan Yin [a], Ethan J. Goodman [a], Lynde M. Wangler [a], Amara C. Davis [a], Braedan T. Oliver [d], Jonathan P. Godbout [a,c,d,*], John F. Sheridan [a,b,c,d,**]

[a] Department of Neuroscience, The Ohio State University Wexner Medical Center, USA
[b] Division of Biosciences, The Ohio State University College of Dentistry, USA
[c] Chronic Brain Injury Program, The Ohio State University, USA
[d] Institute for Behavioral Medicine Research, The Ohio State University Wexner Medical Center, USA

ARTICLE INFO

Keywords:
Stress
RiboTag
Projection neurons to the hippocampus
Anxiety
RNAseq

ABSTRACT

Chronic stress increases the incidence of psychiatric disorders including anxiety, depression, and posttraumatic stress disorder. Repeated Social Defeat (RSD) in mice recapitulates several key physiological, immune, and behavioral changes evident after chronic stress in humans. For instance, neurons in the prefrontal cortex, amygdala, and hippocampus are involved in the interpretation of and response to fear and threatful stimuli after RSD. Therefore, the purpose of this study was to determine how stress influenced the RNA profile of hippocampal neurons and neurons that project into the hippocampus from threat appraisal centers. Here, RSD increased anxiety-like behavior in the elevated plus maze and reduced hippocampal-dependent novel object location memory in male mice. Next, pan-neuronal (Baf53 b-Cre) RiboTag mice were generated to capture ribosomal bound mRNA (i.e., active translation) activated by RSD in the hippocampus. RNAseq revealed that there were 1694 differentially expressed genes (DEGs) in hippocampal neurons after RSD. These DEGs were associated with an increase in oxidative stress, synaptic long-term potentiation, and neuroinflammatory signaling. To further examine region-specific neural circuitry associated with fear and anxiety, a retrograde-adeno-associated-virus (AAV2rg) expressing Cre-recombinase was injected into the hippocampus of male RiboTag mice. This induced expression of a hemagglutinin epitope in neurons that project into the hippocampus. These AAV2rg-RiboTag mice were subjected to RSD and ribosomal-bound mRNA was collected from the amygdala for RNA-sequencing. RSD induced 677 DEGs from amygdala projections. Amygdala neurons that project into the hippocampus had RNA profiles associated with increased synaptogenesis, interleukin-1 signaling, nitric oxide, and reactive oxygen species production. Using a similar approach, there were 1132 DEGs in neurons that project from the prefrontal cortex. These prefrontal cortex neurons had RNA profiles associated with increased synaptogenesis, integrin signaling, and dopamine feedback signaling after RSD. Collectively, there were unique RNA profiles of stress-influenced projection neurons and these profiles were associated with hippocampal-dependent behavioral and cognitive deficits.

1. Introduction

Chronic stress contributes to the development of psychiatric disorders including generalized anxiety disorder, major depressive disorder, and post-traumatic stress disorder (PTSD). Moreover, traumatic or chronic stressors induce stress sensitization (Biltz et al., 2022). Stress sensitization in individuals, increases their vulnerability to negative health consequences, including cognitive dysfunction, after stress (Harkness et al., 2015; McEwen, 2013). These cognitive impairments are associated with neuroanatomical changes and altered connectivity in brains regions involved in fear and memory responses (Mah et al., 2016; Weger and Sandi, 2018). Specifically, there is evidence that the amygdala, a region responsible for emotion and fear control, is hyperactive in individuals with high anxiety. This contributes to increased anxiety and an exaggerated perception of ordinary external stimuli as threats (Stuijfzand et al., 2018). Additionally, hyperactivity in the amygdala

* Corresponding author. Institute for Behavioral Medicine Research Building, 460 Medical Center Drive, Columbus, OH, 43210, USA.
** Corresponding author. Department of Neuroscience, The Ohio State University Wexner Medical Center, USA.
E-mail addresses: Jonathan.Godbout@osumc.edu (J.P. Godbout), John.Sheridan@osumc.edu (J.F. Sheridan).

https://doi.org/10.1016/j.bbih.2024.100908
Received 29 August 2024; Received in revised form 12 November 2024; Accepted 21 November 2024
Available online 29 November 2024

affects the firing of neurons in other brain regions, including the ventromedial prefrontal cortex (vmPFC) and the hippocampus (Bijsterbosch et al., 2015). This is evident in individuals with PTSD who have decreased volume, activation, and connectivity in the hippocampus (Malivoire et al., 2018). These findings indicate that connectivity in stress-responsive regions including the hippocampus, amygdala, and prefrontal cortex contribute to emotional and cognitive impairments that are associated with the development of anxiety, depression, and PTSD.

Repeated social defeat (RSD), a preclinical model of chronic stress, recapitulates physiological, inflammatory, and behavioral consequences similar to individuals with anxiety or depression (Cole et al., 2010; Kiecolt-Glaser and Glaser, 2002). Our previous work shows that RSD activates neurons in stress responsive regions including the prefrontal cortex, amygdala, hippocampus, and hypothalamus (McKim et al., 2018; Wohleb et al., 2011). These regions are associated with fear, interpreting threat stimuli, and memory formation (Martinez et al., 2002; Tovote et al., 2015). Notably, when mice were exposed to acute defeat 24 days after the initial RSD, hippocampal and prelimbic neurons had increased phospho-CREB (p-CREB) expression (DiSabato et al., 2022; Weber et al., 2019). Increased expression of pCREB is implicated in learning-induced synaptic plasticity and may indicate increased neuronal reactivity to threatening stimuli (Bilodeau and Schwendt, 2016; Kivinummi et al., 2011; Tropea et al., 2008). Furthermore, RSD causes anxiety-like behavior (e.g., open field, light/dark preference), social withdrawal, social avoidance, increased fear expression, and cognitive deficits (e.g., Morris water maze and Barnes maze) (DiSabato et al., 2021; McKim et al., 2016, 2018; Wohleb et al., 2011, 2013). Social avoidance and prolonged fear expression persisted following the cessation of RSD (Goodman et al., 2024; Lisboa et al., 2018; Wohleb et al., 2014a). Similarly, individuals with PTSD showed impaired recall following fear extinction with increased activation in the amygdala and decreased activation in the hippocampus and prefrontal cortex during recall (Milad et al., 2009). Therefore, the connections between the amygdala, prefrontal cortex, and hippocampus are important for behavioral and cognitive deficits induced by stress.

The hippocampus is critical for memory and the interpretation of fear and threat after RSD (DiSabato et al., 2021; McKim et al., 2016). Previous studies of RSD in mice show that the hippocampus had a robust immune profile associated with interleukin (IL)-1β signaling, microglia reactivity, and a reactive endothelium (DiSabato et al., 2021; McKim et al., 2018; Sawicki et al., 2015; Wohleb et al., 2013; Yin et al., 2022). As mentioned, chronic stressors like RSD result in neuronal sensitization within the prefrontal cortex, amygdala, and hippocampus (Weber et al., 2019). The regions interact in a complex and highly interconnected manner to impact learning and memory consolidation after a fearful stimuli or stressful event (Lesting et al., 2011; Sierra-Mercado et al., 2011; Zelikowsky et al., 2014). Evidence indicates that chronic stress shifts the excitatory-inhibitory (E-I) balance within the prefrontal cortex and amygdala to the hippocampus and results in a shift in communication (Zelikowsky et al., 2013). Furthermore, the hippocampus is integral in synaptic plasticity and memory formation (Martinez et al., 2002; Shin and Liberzon, 2010; Tovote et al., 2015). The hippocampus receives direct inputs from various regions including the amygdala, which provides critical input and regulates fear responses to aggressive stimuli (Shin and Liberzon, 2010). There is preclinical evidence that the fear and memory circuit influence behavioral responses. For instance, the basolateral amygdala (BLA) and the hippocampus become activated in anxious mice experiencing morphine withdrawal (Deji et al., 2022). Inhibiting projections from BLA to the hippocampus prevented the development of anxiety-like behavior in those same mice (Deji et al., 2022). Additionally, the hippocampus projects monosynaptically to the prefrontal cortex, while the prefrontal cortex indirectly projects to the hippocampus through the thalamic reuniens (RE) (Goswamee et al., 2021; Vertes et al., 2007). There is evidence that these circuits play a critical role in fear recall and learning (Ortiz et al., 2019; Ramanathan et al., 2018; Xu and Sudhof, 2013). For example, silencing the projections from the medial prefrontal cortex to the RE impaired the expression of fear extinction (Ramanathan et al., 2018). Moreover, lesions or silencing in the RE impaired spatial working memory (Hallock et al., 2016; Ito et al., 2015). These findings provide support for the notion that projections from the prefrontal cortex to hippocampus play a pivotal role in memory formation and recall. Therefore, the intricate neuronal circuitry between stress-responsive brain regions may influence chronic anxiety and memory deficits.

The purpose of this study was to determine the transcriptional signature of neurons within the hippocampus and prefrontal cortex and neurons that project into to the hippocampus from the amygdala. We aimed to increase our understanding of pathways activated in neurons after social defeat that may underlie stress sensitization. Here, we identified that RSD-induced a unique pattern of gene expression within cortical projection neurons and neurons that project to the hippocampus from the amygdala using the RiboTag approach (Sanz et al., 2009) and retrograde viral tracing.

2. Methods

Mice: Male wild type C57BL/6 mice (6–8 wks) were purchased from Charles River Laboratories (Wilmington, MA). Pan-neuronal RiboTag mice were bred in-house by crossing male Baf53 b-Cre (B6.Cg-Tg (Actl6b-Cre)4092Jiwu; Jax strain #027826) with female RiboTag mice (B6N.129-Rpl22tm1.1Psam/J; Jax strain # 011029). Baf53 b-Cre^{+} RiboTag males were used as experimental mice. Neuronal-specific RiboTag mice were generated by crossing Rpl22-StoploxP/loxP-Hemagglutinin (HA) mice with a pan-neuronal-specific Baf53 b-Cre^{+} mice. For the retrograde AAV experiments, male RiboTag (B6N.129-Rpl22tm1.1Psam/J; Jax strain # 011029) mice were injected (0.5 μl) bilaterally into the CA1 region of the hippocampus with pENN.AAV2rg.hSyn.HI.eGFP-Cre.WPRE.SV40 (AAV2rg). Experimental wild-type and transgenic mice were housed 3 per cage. CD-1 retired breeders (12 months) were purchased from Charles River Laboratories (Wilmington, MA) and housed individually. All mice were housed in 11.5″x 7.5″x 6″ polypropylene cages and provided with food and water ad libitum. Rooms were maintained at 21 °C under a 12 h light/dark cycle with the light cycle beginning at 06:00. Experimental mice were randomly selected for RSD or Control and were evenly distributed. All procedures were in accordance with the NIH Guidelines and were approved by the Ohio State University Institutional Laboratory Animal Care and Use Committee.

Repeated Social Defeat (RSD): Mice were subjected to Repeated Social Defeat (RSD) as previously described (Wohleb et al., 2013). In brief, a CD-1 aggressor mouse was placed into each of the home cages of experimental mice for 2 h (between 16:00 to 18:00) each day for six consecutive days. During the 2 h, submissive behaviors (e.g., upright posture, crouching) were observed to ensure experimental mice showed signs of defeat. A new CD-1 aggressor was introduced to the cage if no attack occurred within 3–5 min or if an experimental mouse defeated the CD-1 aggressor. At the end of the 2 h period, aggressor mice were removed, and experimental mice were left undisturbed in their home cages until the following day when the protocol was repeated. To avoid habituation, different aggressors were used on consecutive days. The health of the experimental mice was monitored carefully throughout the experiments. Experimental mice that were significantly wounded, injured, or moribund were removed from the study. Similar to previous studies, less than 5% of mice met the early removal criteria (Wohleb et al., 2011). Control mice were left undisturbed in a separate room and in their home cages.

Elevated Plus Maze: Fourteen hours after RSD, wild-type mice were subjected to elevated plus maze. Mice were habituated to the behavior room for 30 min prior to testing. At the start, mice were placed in the center of the elevated plus maze facing the open arm. Mice were tested one at a time and activity was recorded for 5 min. Automated tracking

software (Ethovision (v13)) was used to determine several parameters including total distance travelled, the number of visits into the arms (open and closed), and the time spent in each arm (open or closed). All trials were recorded and analyzed by an investigator who was blind to the treatment groups (Control and Stress).

Novel Object Recognition and Location Memory: Novel object recognition (NOR) and novel object location (NOL) memory tasks were performed with wild-type mice as previously described (Bray et al., 2022; Wangler et al., 2022; Witcher et al., 2021). In brief, experimental mice underwent four 10 min trials with 24-h intertrial intervals over four days: habituation (no objects), acquisition (two different objects), recognition testing (two different objects, with one novel object), and location testing (two objects that were used from previous day, with one object in new location) beginning 14 h after repeated social defeat. NOR/NOL were performed under ambient lighting with corn cob bedding. Total time of exploration [(TTE) = timenovel + timefamiliar] and percentage of time spent with novel (timenovel/TTE × 100) were calculated for both NOR and NOL memory trials (Denninger et al., 2018). All trials were recorded and analyzed by an investigator who was blind to the treatment groups (Control and Stress).

Retrograde AAV2-Cre injection: Male RiboTag mice (4-week-old) underwent stereotaxic surgery for bilateral injection (0.5 μl) of pENN.AAV2rg.hSyn.HI.eGFP-Cre.WPRE.SV40 (Addgene, #105540-AAV2rg) into the CA1 of the hippocampus bilaterally (−1.82 AP, ± 1.57 ML, 1.85 DV). Mice were left undisturbed for four weeks prior to starting RSD. All injections were performed by the same investigator using the same virus vial, amount, and location. Immunohistochemistry was used to confirm inject site and transfection.

RiboTag HA-immunoprecipitation: For all bulk-RNA sequencing experiments, immunoprecipitation of polysome-bound mRNA from hippocampal neurons were performed in Baf53 b-Cre Rpl22-HA mice (hippocampal microdissections) and from the prefrontal cortical and amygdala neurons in AAVrg-RiboTag mice as previously described (Yin et al., 2022). In brief, brain regions were dissected 14 h after RSD and snap frozen in liquid nitrogen until immunoprecipitation. Microdissections were homogenized (Dounce homogenizer) using ice-cold buffer containing 1% Nonidet-P40, 100 mM KCl, 50 mM Tris pH 7.4, 12 mM $MgCl_2$, 0.1 mg/ml cycloheximide, 1:100 protease inhibitor, 200 U/ml RNasin, and 1 mM DTT. Homogenates were clarified by centrifugation (10,000×*g* for 10 min). The resulting supernatant from each sample was incubated with Protein A/G magnetic beads (Thermo Fisher, cat #8803) for 30 min on a rotator. Next, the precleared lysate (i.e., purified samples) was incubated with anti-HA (Biolegend cat#901515) for 4 h at 4 °C. Next, the purified samples with anti-HA were added to prewashed Protein A/G magnetic beads and incubated at 4 °C for 8 h. Finally, the beads were washed 3x with a high salt elution buffer (1% Nonidet-P40, 300 mM KCl, 50 mM Tris, 12 mM MgCl2, 1 mM DTT, 0.1 mg/ml cycloheximide, 100 U/ml RNasin, 1:200 protease inhibitor) and RNA was collected using Buffer RLT with beta-mercaptoethanol (RNeasy Micro Kit, Qiagen, cat# 74004). RNA was isolated using the RNeasy Micro Kit according to manufacturer's instructions.

Immunofluorescence: HA was labeled as previously described (Yin et al., 2022). Fourteen hours after RSD, mice were transcardially perfused with ice-cold PBS (pH 7.4) followed by 4% formaldehyde. Brain samples were post-fixed for 24 h, cryoprotected in 30% sucrose for 24 h, frozen at −80 °C, sectioned (30 μm), and stored in cryoprotectant at −20 °C until use. Brain regions were identified using the Allen Mouse Brain Atlas (Allen Institute). Sections were washed in PBS, blocked (with solution containing 10% normal donkey serum, 1% bovine serum albumin, and 0.1% TritonX in PBS) for 2 h, and incubated with primary antibodies: guinea pig anti-mouse PV antibody (1:500; Synaptic Systems, #195004, Synaptic Systems) and rabbit anti-mouse HA (1:500; Cell Signaling, cat# 3725 S). Sections were incubated overnight at 4 °C. Next, sections were washed in PBS and incubated with an appropriate fluorochrome-conjugated secondary antibody for 1 h (1:500; Donkey anti-rabbit, AlexaFluor 647; Donkey anti-chicken, AlexaFluor 594; Thermo Fisher Scientific). Sections were mounted on charged slides, cover-slipped and counterstained with DAPI and stored at −20 °C. Slides were visualized and imaged using an EVOS M7000 imaging system (Thermo Fisher Scientific) at 4X and 10× magnification. For ΔFosB, cells with positive labeling were counted in each section using ImageJ. Values from 2 to 3 images per mouse were averaged, and these values were used to calculate group averages and variance for each experimental group for HA and PV (DiSabato et al., 2022; Yin et al., 2022). Investigators were blind to experimental groups prior to all microscopy and image analysis.

RNAseq: Quality control for RiboTag samples was performed using the PicoAssay by Chip (Agilent) and samples with RIN >8.0 were processed for sequencing. Each mouse represents one biological sample and was not combined. Amygdala cDNA libraries were generated with the Ovation SoLo RNA-Seq System (NuGEN) and sequenced at a depth of 40 M single-end bp100 reads per sample. Hippocampi and prefrontal cortices cDNA libraries were generated with the NovaSeq 6000 (Illumina) and sequenced at a depth of 40 M paired end bp150 reads per sample. Amygdala library preparation and sequencing were conducted at the University of Miami (Center for Genome Technology (CGT), John P. Hussman Institute for Human Genomics, University of Miami Miller School of Medicine, Miami, FL. Hippocampi and prefrontal cortex library preparation and sequencing were conducted at Novogene (Sacramento, CA). For all regions, data were aligned to the mouse mm10 reference genome using STAR aligner as previously described (Yin et al., 2022). Differential expression of genes was analyzed using the DESeq2 package in R. Differentially expressed genes were those with a p-value below 0.05. Stratified Rank-Rank hypergeometric plots were made with RRHO2 package in R. To generate the same gene list, DEGs from all three data sets were combined the plots. The respective p-values and fold changes were used for each gene. DDE was calculated as -log10(pvlaue) * sign(effect size). Pathway analysis was performed using Ingenuity Pathway Analysis (Qiagen). Results of IPA, including DEGs listed for each pathway, were considered significant with $p < 0.05$ and z score >2. Relationships between gene changes were visualized using Cytoscape EnrichmentMap app of Gene Ontology (GO) cellular compartments and biological processes with Q-value cutoff of 0.1.

Statistical Analysis: Behavioral testing was analyzed with an unpaired parametric *t*-test on GraphPad Prism 9. Data are expressed as mean ± standard error of the mean (SEM). Threshold for statistical significance (*) was set at $p < 0.05$. Tendency for significance was considered when the p value was in the range of $p = 0.06–0.10$. Individual data points that fell more than two standard deviations above and below the mean were considered outliers and were excluded in the subsequent analyses.

3. Results

3.1. Repeated social defeat increased anxiety-like behavior and memory deficits

Repeated social defeat in mice causes anxiety-like behavior (e.g., open field, light/dark preference), social withdrawal, and cognitive deficits (e.g., Morris water maze and Barnes maze) (McKim et al., 2016; Wohleb et al., 2013). The connections between the amygdala and hippocampus and the prefrontal cortex to hippocampus are important for the anxiety-like and cognitive deficits induced by stress. For instance, the elevated plus maze (EPM) is an amygdala-hippocampal relevant task and NOR/NOL are cortical-hippocampal and amygdala-hippocampal relevant memory assessments (Barsegyan et al., 2014; Denninger et al., 2018; Silveira et al., 1993; Walf and Frye, 2007). Thus, the two initial experiments assessed anxiety-like behavior during the EPM and memory deficits on NOR/NOL testing after RSD.

In two independent experiments, EPM and NOR/NOL were assessed 14 h after RSD (Fig. 1A). In the EPM experiment (Fig. 1B), the total distance travelled during testing was unaffected by RSD (Fig. 1C). In

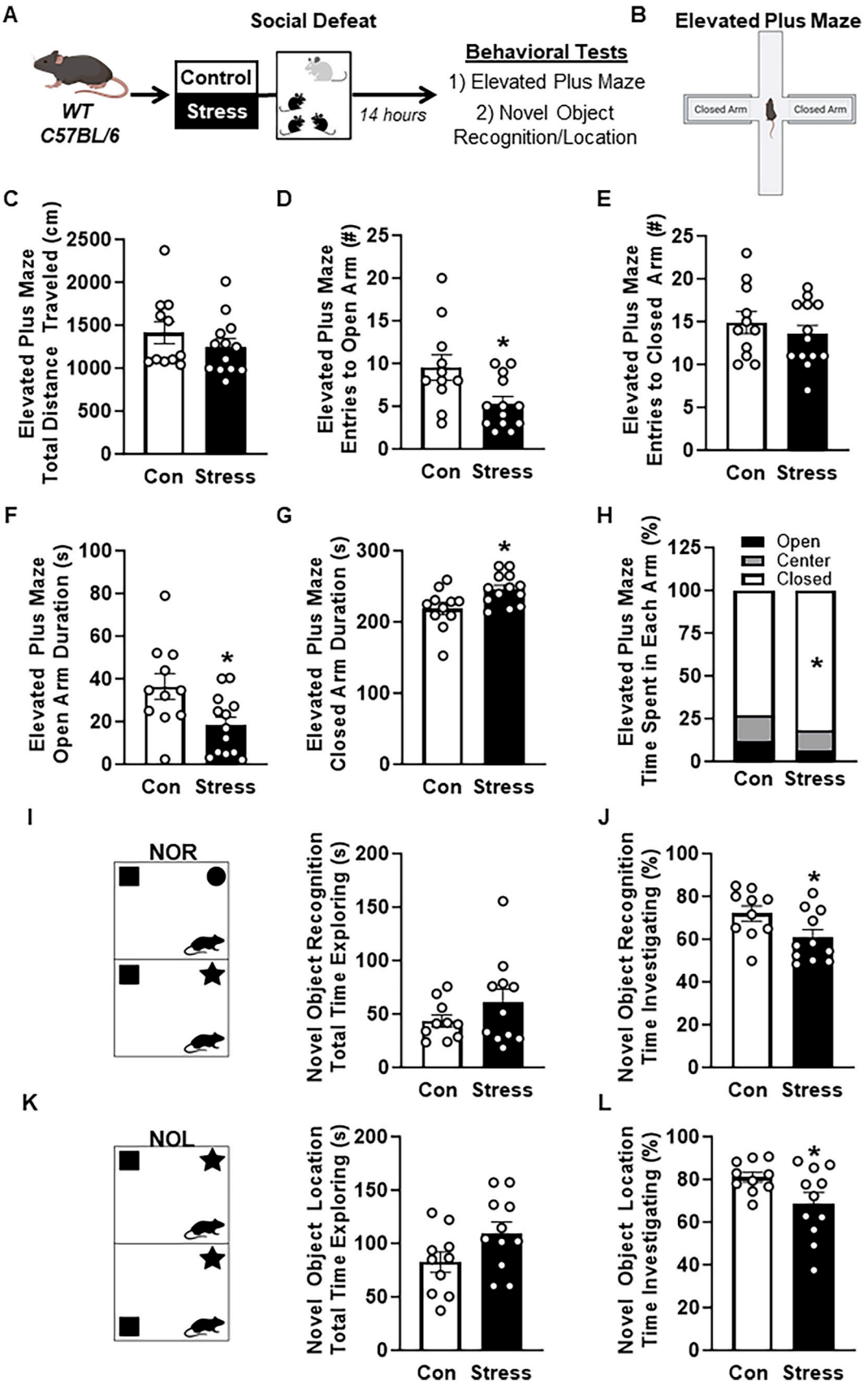

(caption on next page)

Fig. 1. Repeated Social Defeat increased anxiety-like behavior and memory deficits. A) Male wild type C57BL/6 mice were subjected to repeated social defeat (Stress) or left undisturbed (Con). Anxiety-like behavior or cognition was assessed 14 h later in two independent experiments. **B)** For the elevated plus maze (EPM), mice were placed in the EPM for 5 min to determine anxiety-like behavior (n = 11–13). **C)** Total distance travelled in the EPM. **D)** The number of entries into the open arm during EPM. **E)** The number of entries into the closed arm during EPM. **F)** Duration in the open arm during EPM. **G)** Duration in the closed arm during EPM. **H)** Percent time spent in the three areas of the EPM: center, open arms, and closed arms. In a separate experiment, novel object recognition (NOR) and novel object location (NOL) were used to assess hippocampal dependent memory after RSD (n = 10–11). **I)** Schematic of NOR and total time exploring during testing. **J)** Percentage of time spent investigating the novel object during NOR. **K)** Schematic of NOL and total time exploring during testing. **L)** Percentage of time spent investigating the novel location during NOL. Bars represent the mean ± SEM, and individual data points are provided. Means with asterisk (*) are significantly different from Controls ($p < 0.05$).

addition, RSD decreased the number of entries in the open arm ($p = 0.0165$, Fig. 1D). The number of entries into the closed arm of the EPM was not different between control and RSD (Fig. 1E). RSD decreased the duration of time spent in the open arm of the EPM ($p = 0.0159$, Fig. 1F). RSD increased the time spent in the closed arm ($p = 0.015$, Fig. 1G). Total percentage of time in the open ($p = 0.0154$), closed ($p = 0.0196$), and center of the EPM are shown (Fig. 1H). These data indicate that RSD increased anxiety-like behavior in the EPM.

In the second experiment, novel object recognition (NOR) and novel object location (NOL) memory testing began 14 h after RSD (Fig. 1A). In the NOR test (3 days after RSD concluded), there were no differences between control and RSD mice in total time exploring the objects (Fig. 1I). In addition, RSD decreased the amount of time investigating the novel object compared to controls ($p = 0.0387$, Fig. 1J). NOL testing was assessed 24 h after NOR (4 days after RSD concluded, Fig. 1K). In the NOL, the total time exploring the objects between control and RSD mice was not different (Fig. 1K). The percent time investigating the object in the novel location, however, was reduced by RSD compared to controls ($p = 0.045$, Fig. 1L). Taken together, RSD increased learning and memory deficits associated with the cortex and hippocampus.

3.2. Repeated social defeat increased expression of genes associated with neuroinflammation, synaptic long-term potentiation, oxidative phosphorylation, and Gαs signaling in hippocampal neurons

The hippocampus is critical for memory and the interpretation of fear and threat after RSD (Biltz et al., 2024; DiSabato et al., 2021; Goodman et al., 2024; McKim et al., 2016). Previous studies of RSD in mice show that the hippocampus had an increased immune profile associated with interleukin (IL)-1β signaling, microglia reactivity, and a reactive endothelium (DiSabato et al., 2021; McKim et al., 2018; Sawicki et al., 2015; Wohleb et al., 2013; Yin et al., 2022). In this experiment, we aimed to determine the RNA profile of activated neurons in the hippocampus after RSD. Here, neuron specific Cre + -RiboTag mice were generated by crossing Rpl22-Stop$^{loxP/loxP}$-Hemagglutinin (HA) mice with a pan-neuronal-specific Baf53 b-Cre^{+} mice (Fig. 2A). HA expression was confirmed in neurons (NeuN^{+}, Fig. 2B). Next, Baf53b/Rpl22-HA mice were subjected to RSD and neuron-specific mRNA was collected from the hippocampus. The isolated RNA was sequenced and DEGs were determined (Fig. 2C). There were 1632 DEGs after RSD (884 increased, 748 decreased) in hippocampal neurons (Fig. 2D–E, $p < 0.05$).

Next, Ingenuity Pathway Analysis (IPA) was used to determine canonical pathways influenced by RSD in the "Ribotagged" neurons within the hippocampus (Fig. 2F). RSD increased several canonical signaling pathways (number of related DEG's listed for each pathway) including Oxidative phosphorylation, Ceramide signaling, Synaptic Long-term Potentiation, Reelin signaling, c-AMP signaling, and NfκB/neuroinflammatory signaling (>2 Z-score, $p < 0.05$, Fig. 2F). Canonical pathways that were decreased in hippocampal "Ribotagged" neurons after RSD included Sirtuin Signaling, Calcium Signaling, and Mitochondrial dysfunction (>2 Z-score, $p < 0.05$, Fig. 2F). The DEGs associated with these pathways are highlighted in the heat maps ($p < 0.05$, Fig. 2G and H). For instance, RSD increased 9 DEGs (e.g., *Mras, Crhr1, Grm2*) and decreased 6 DEGs (e.g., *Prkcd, Cacmg6*) associated with synaptic long-term potentiation. Additionally, RSD increased 9 DEGs (e.g., *Adra2c, Grm2, Chrm5*) and decreased 5 DEGs (e.g., *Rgs14, Camk4*) involved in cAMP signaling. Similarly, RSD increased 6 DEGs (e.g., *Adcy6, Crhr1, Chrm5*) and decreased 4 DEGs (e.g., *Gnb4*) that are associated with Gαs Signaling. There were 18 DEGs (5 increased, 13 decreased) that were associated with reduced calcium signaling after RSD (e.g., *Mef2a, Camk4*). Taken together, RSD increased DEGs in hippocampal "Ribotagged" neurons that are associated with increased synaptic LTP, neuroinflammation, cAMP signaling, and Gαs signaling.

Next, DEGs that were affected by stress, both increased and decreased, were input into Cytoscape EnrichmentMap to visualize Gene Ontology (GO) Cellular Compartment and Biological Processes. Stress increased the number of DEGs associated with synapses, glutamatergic synapses, cell junction, neuronal projection, and postsynaptic density (Fig. 3A) in hippocampal neurons. Stress increased the number of DEGs associated with neurogenesis, neuron development, cell projection organization, and neuron projection development (Fig. 3B) in hippocampal neurons.

3.3. Viral tracing of neurons in the amygdala that project into the hippocampus

The hippocampus receives inputs (indirectly and directly) from regions associated with fear and threat appraisal (Dolleman-van der Weel et al., 2019; Felix-Ortiz et al., 2013; Goswamee et al., 2021; Lesting et al., 2011; Vertes et al., 2007). Thus, the purpose of this experiment was to trace neurons that project from the basolateral amygdala (directly) to the hippocampus. Here, RiboTag mice (*Rpl22*-Stop$^{loxP/loxP}$)-Hemagglutinin (HA) were injected bilaterally into the CA1 of the hippocampus with a retrograde-adeno-associated virus (AAV2rg--Cre-GFP, Fig. 4A) to induce recombination and subsequent expression of HA in neurons that project into the hippocampus (Fig. 4B). AAV2rg (GFP^{+}). Notably, this AAV2rg-Cre virus is monosynaptic. HA^{+} expression was confirmed in regions of the hippocampus (e.g., dentate gyrus) that project to the CA1 four weeks after AAV2rg injection (Fig. 4C). Next, HA^{+} neurons were visualized in the amygdala (Fig. 4D). Thus, neurons in the basolateral amygdala project directly to the hippocampus.

Next, labeling for HA and parvalbumin (PV) expression was determined in neurons within the amygdala (Fig. 4E). These images illustrate that HA labeling within the amygdala that was independent of PV labeling. Therefore, the interpretation is that these connections are likely excitatory and not GABAergic (inhibitory).

3.4. Repeated social defeat increased expression of genes associated with synaptogenesis and neuroinflammation in neurons that project from the amygdala to the hippocampus

Similar to the above approach, we aimed to capture neurons that project directly from the amygdala to the hippocampus. Again, RiboTag mice were injected with AAV2rg-Cre into the CA1 of the hippocampus. Four weeks later, mice were subjected to RSD, RNA from HA-tagged activated neurons in the amygdala was immunoprecipitated (Fig. 5A) and neuronal RNA was isolated and sequenced. There were 627 DEGs (416 increased, 211 decreased) in neurons that project from the amygdala into the hippocampus (Fig. 5B–C, $p < 0.05$). IPA determined canonical pathways that were increased in neurons included Integrin Signaling, Cytokine Storm Signaling, IL-4 signaling, Synaptic LTP,

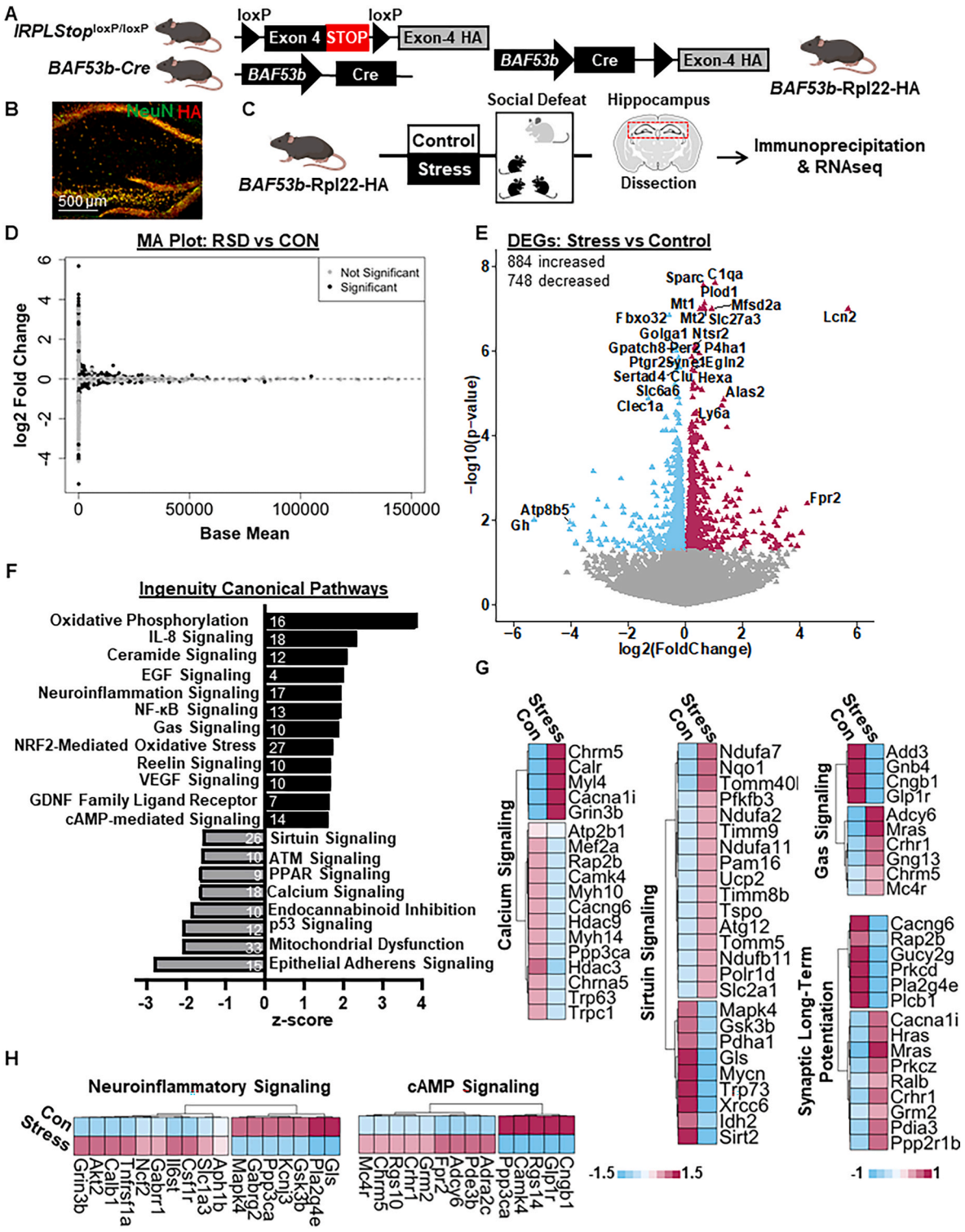

Fig. 2. Repeated Social Defeat influenced the RNA profile of hippocampal neurons with DEGs associated with neuroinflammation, synaptic long-term potentiation, oxidative phosphorylation, and Gαs signaling. A) Schematic of the generation of Baf53b/Rpl22-HA (Pan-neuronal RiboTag) mice. **B)** Representative images of NeuN (green) and HA (red) labeling in the hippocampus of Cre $^{+}$ RiboTag mice. **C)** Experimental design with male Cre^{+} Baf53b/Rpl22-HA (Pan-neuronal RiboTag) mice subjected to repeated social defeat (Stress) or left undisturbed (Con). Fourteen hours after RSD, the brain was collected, hippocampi (HPC) were dissected, polysome-bound neuronal mRNA was immunoprecipitated, and RNA was sequenced (n = 6). **D)** MA plot of differentially expressed genes (DEGs) in the hippocampus. The black dots represent significant genes ($p < 0.05$). **E)** Volcano plot of DEGs in the hippocampus of Stress and Control. The blue triangles represent genes that were significantly decreased with Stress |log2FoldChange| >0. The pink triangles represent genes that were significantly increased with Stress | log2FoldChange| > 0. **F)** Ingenuity Pathway Analysis of canonical pathways inhibited or activated by stress compared to control in the hippocampus (|z-score| > 1.5). Number of DEGs associated with each pathway are represented in the bar corresponding to that pathway. **G-H)** Heat map of DEGs ($p < 0.05$) in the hippocampus associated with calcium signaling, sirtuin signaling, oxidative phosphorylation, Gαs signaling, synaptic long-term potentiation, and neuroinflammation, and cAMP signaling determined by Ingenuity Pathway Analysis. (For interpretation of the references to color in this figure legend, the reader is referred to the Web version of this article.)

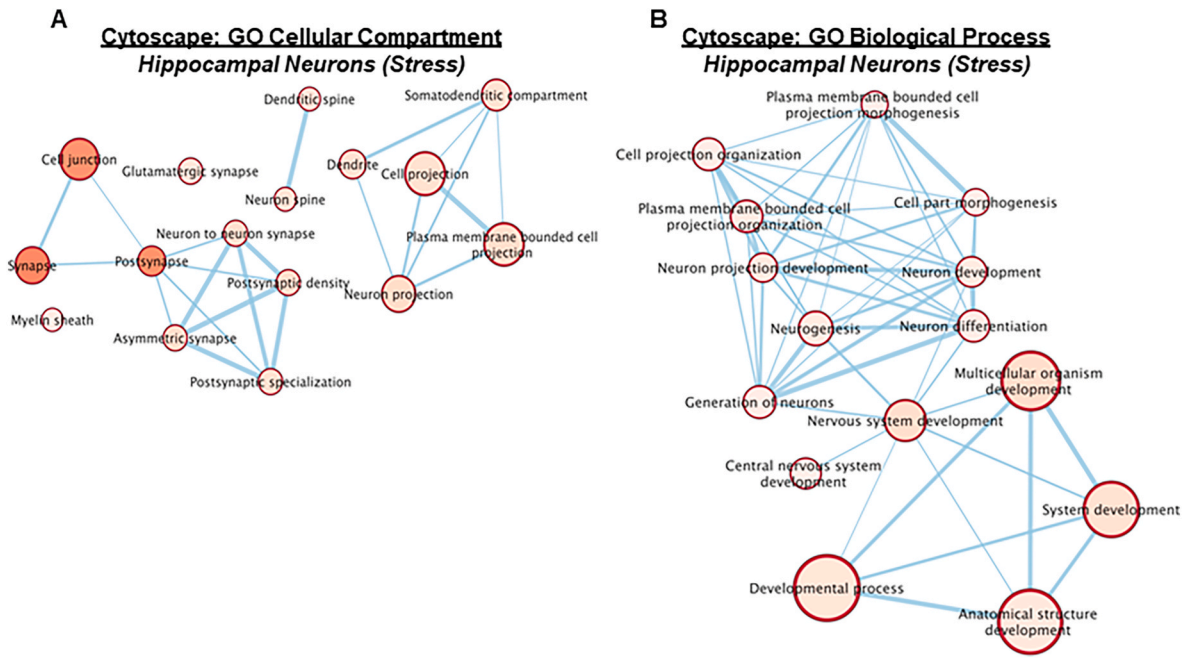

Fig. 3. Enrichment maps of cellular compartments and biological processes in hippocampal neurons after Repeated Social Defeat. A) Gene Ontology Cellular Compartment determined by Cytoscape EnrichmentMap (CEM) that were affected in hippocampal neurons after Stress. Circle size represents the number of genes within the category and the color of the circle represents the relative strength of connections. **B)** Gene Ontology Biological Process determined by Cytoscape EnrichmentMap (CEM) that affected in hippocampal neurons after Stress. Circle size represents the number of genes within the category and the color of the circle represents the relative strength of connections. (For interpretation of the references to color in this figure legend, the reader is referred to the Web version of this article.)

Synaptogenesis, and Dopamine Signaling (>2 z-score, $p < 0.05$, Fig. 5D). Canonical pathways decreased after RSD included RHOGDI Signaling, PTEN Signaling, CREB Signaling, and PPAR Signaling (>2 z-score, $p < 0.05$, Fig. 5E). RSD increased 13 DEGs (e.g., *Arpc1b, Adcy4*) and decreased 11 DEGs (e.g., *Gna12, Ryr1*) associated with synaptogenesis ($p < 0.05$, Fig. 4E). Additionally, RSD decreased genes associated CREB signaling (e.g., *Adra2b, Gna12, Gpr139)* and increased neuroinflammation (e.g., *Il-1r1, Il18rap, Tnfrsf1a),* oxidative phosphorylation, nitric oxide, and reactive oxygen species production (e.g., *Vegfa, S110a8)* in the amygdala ($p < 0.05$, Fig. 5F). RSD increased 4 DEGs (e.g., *Acta2, Xbp1)* and decreased 7 DEGs (e.g., *Gsk3b, Aldh1a1)* involved with mitochondria dysfunction ($p < 0.05$, Fig. 5F). Collectively, RSD induced a unique gene expression profile in neurons that project from the basolateral amygdala to the hippocampus that was associated with synaptogenesis, actin cytoskeleton signaling, neuroinflammation, nitric oxide, and oxidative phosphorylation.

Next, DEGs increased by stress were input into Cytoscape EnrichmentMap to visualize Gene Ontology (GO) Cellular Compartment and Biological Processes. Stress increased the number of DEGs associated with intracellular structure and neuronal projection, synapses, and cell junction (Fig. 6A) in amygdala projection neurons. For GO Biological processes (Fig. 6B), stress increased the number of DEGs associated with cell projection organization, cell development, receptor signaling, and response to cytokine stimulus in amygdala projection neurons.

3.5. Repeated social defeat increased expression of genes associated with synaptogenesis, integrin signaling, and dopaminergic signaling in prefrontal cortex projection neurons

Here, we aimed to capture and sequence neurons that project from the prefrontal cortex to the hippocampus. Using the same approach as above, RiboTag mice were injected with AAV2rg-Cre into the CA1 of the hippocampus. Four weeks later, mice were subjected to RSD and RNA from HA-tagged neurons in the prefrontal cortex were immunoprecipitated (Fig. 7A). There were distinct neurons in the prefrontal cortex that were HA positive 4 weeks after AAV2rg injection into the hippocampus (Fig. 7A). Again, this AAV2rg-Cre virus is monosynaptic, so these HA-tagged cortical neurons are likely direct projections to the hippocampus. Nonetheless, it is possible that they are prefrontal cortical projections that were labeled by AAV2rg that leaked in the cortex during injection. Either way, all of these neurons are prefrontal cortical projection neurons that were influenced by stress. Ribosomal-bound RNA from these cortical neurons were captured and sequenced. Thus, this AAV2rg-Cre tracing and capture method in Ribotag mice includes prefrontal cortex neurons that were affected by RSD (Fig. 7C).

There were 1111 differentially expressed genes (DEG, 657 decreased & 454 increased) in prefrontal cortex neurons (Fig. 7D–E, $p < 0.05$) Next, IPA was used to determine canonical pathways activated by stress in these prefrontal cortical projection neurons (Fig. 7F and G). RSD increased canonical signaling pathways (the number of related DEG's listed for each pathway) including VEGF signaling, RAC signaling, Reelin signaling, Synaptogenesis and Dopamine feedback in cAMP signaling (Fig. 7F). Fig. 7G shows canonical pathways inhibited by stress in the prefrontal cortex. RSD decreased canonical signaling pathways including Oxidative Phosphorylation, PTEN Signaling, and p53 Signaling (>2 Z-score, $p < 0.05$, Fig. 7G). The DEGs associated with these pathways are highlighted in the heat maps. For instance, RSD increased 21 genes (e.g., *Pik3r4, Syn1, Syngap1*) and decreased 6 genes (e.g., *Cdh1, Atf4*) associated with synaptogenesis signaling (Fig. 8C). Additionally, there were 20 DEGs (14 increased, 6 decreased) associated with increased integrin signaling (e.g, *Actn2, Pik3r4*) in the prefrontal cortex after RSD. RSD increased 12 DEGs (e.g, *Nos1, Grin2b*) and decreased 7 DEGs (e.g., *Atf4*) involved in dopamine signaling in the prefrontal cortex. Furthermore, there were 27 DEGs (e.g., *Cacna1e, Adcy3*) increased and 10 DEGs (e.g., *Atf4, Yes1*) decreased involved in serotonergic signaling in neurons that project from the prefrontal cortex into the hippocampus. Collectively, gene expression in projection neurons from the prefrontal cortex was associated with increased synaptogenesis, dopaminergic feedback in cAMP signaling, integrin signaling, serotonergic signaling, and oxytocin signaling after RSD.

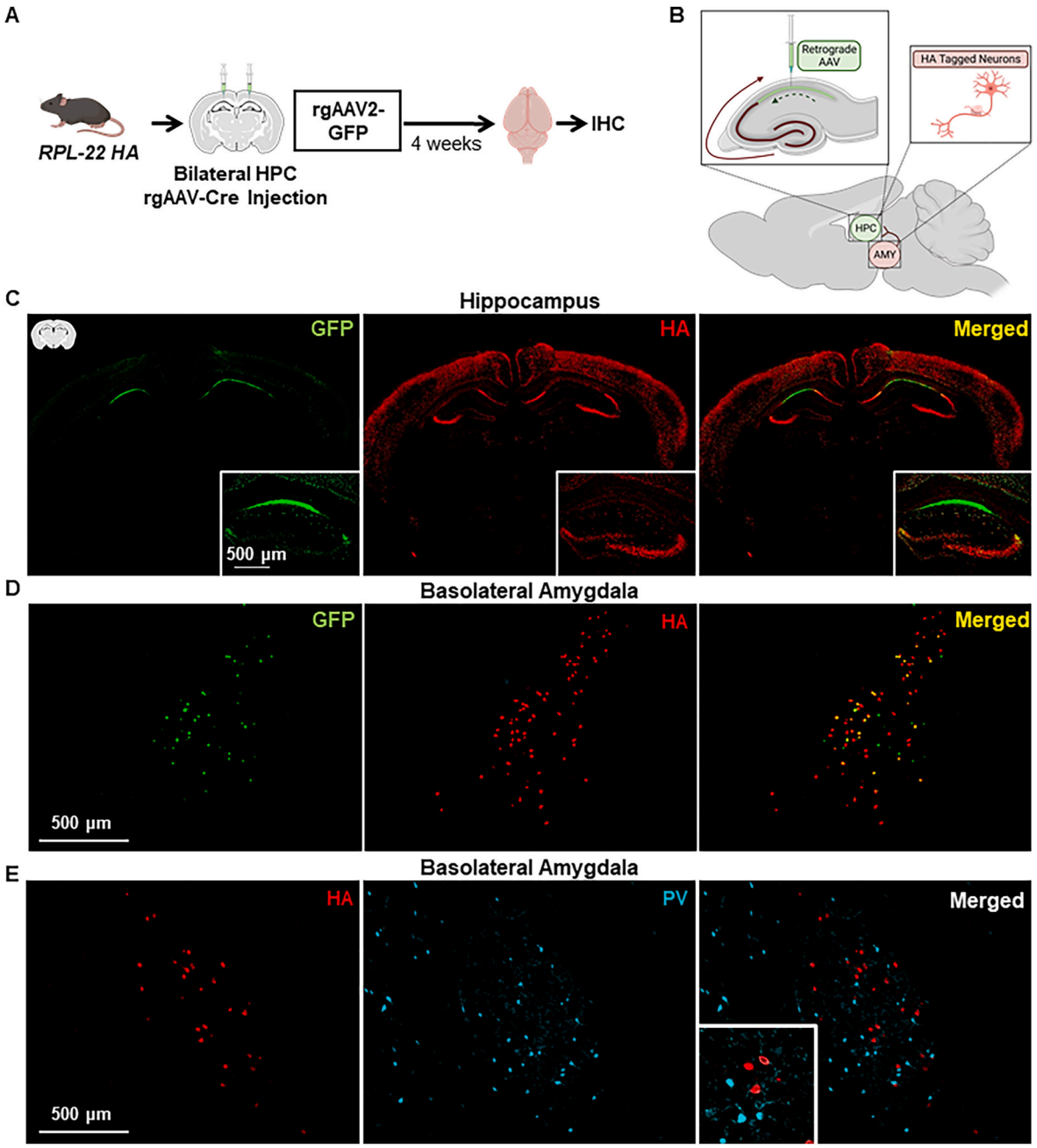

Fig. 4. Tracing of neurons in the amygdala that project to the hippocampus. A) Diagram shows male RiboTag (Rpl22-HA) mice injected bilaterally into the CA1 region of the hippocampus (HPC) with a retrograde (rg) AAV2–Cre (pENN.AAV2rg.hSyn.HI.eGFP-Cre.WPRE.SV40). Brain sections were collected 4 weeks later and expression of AAV2rg and HA were determined (n = 5). **B)** Schematic of rgAAV2-Cre labeling in the hippocampus of RiboTag mice. **C)** Representative images of AAV2rg (green), HA (red), and co-localization (yellow) labeling in a cortex-hippocampal (tile scan, 4x) of AAV2rg-RiboTag mice. Insets are representative images (10x) of AAV2rg (green), HA (red), and co-localization (yellow) labeling in the hippocampus of AAV2rg-RiboTag mice. **D)** Representative images of AAV2rg (green), HA (red), and co-localization (yellow) labeling in the basolateral amygdala (BLA, 10x) of AAV2rg-RiboTag mice. **E)** Representative images of parvalbumin (PV, blue) and HA (red) labeling in the BLA (10x) of AAV2rg-RiboTag mice. (For interpretation of the references to color in this figure legend, the reader is referred to the Web version of this article.)

Next, DEGs increased by stress were input into Cytoscape EnrichmentMap to visualize Gene Ontology (GO) Cellular Compartment and Biological Processes. Stress increased the number of DEGs associated with post synapses, postsynaptic density, neuron projection, axon, and glutamatergic synapses (Fig. 8A) in prefrontal cortex projection neurons. Stress increased the number of DEGs associated with learning, memory, long-term potentiation, post synapse organization and density (Fig. 8B) in prefrontal projection neurons.

Comparison of cortical and amygdala projection neurons after Repeated Social Defeat. To further understand regional differences in the brain after RSD, the RNA sequencing datasets for the neurons that project into the hippocampus from the amygdala (Figs. 5 and 6) and neurons that projection from the prefrontal cortex (Figs. 7 and 8) were compared. The stratified Rank-Rank Plot shows overlap in the concordant quadrants (i.e. genes upregulated and downregulated in both regions) in the prefrontal cortex and amygdala after Stress (Fig. 9A). The Venn diagram in Fig. 9B shows unique and shared DEGs in projection neurons from amygdala to the hippocampus and neurons in the prefrontal cortex. For instance, neurons from the prefrontal cortex had 1077 unique DEGs after RSD compared to the 593 unique DEGs in neurons

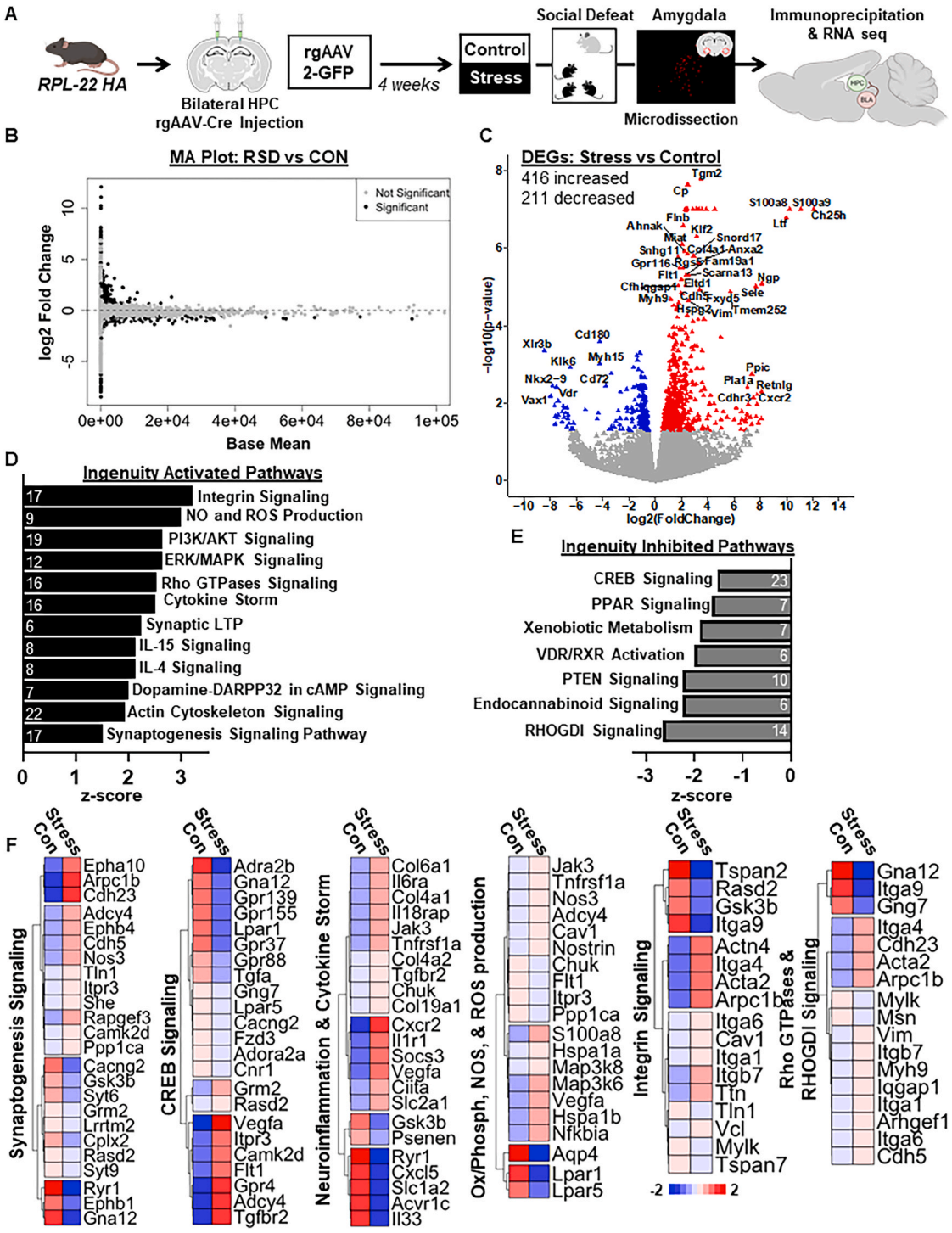

Fig. 5. Repeated Social Defeat increased expression of genes associated with synaptogenesis and neuroinflammation in neurons that project from the amygdala to the hippocampus. A) Diagram shows male RiboTag (Rpl22-HA) mice injected bilaterally into the CA1 region of the hippocampus (HPC) with a retrograde AAV2– Cre (pENN.AAV2rg.hSyn.HI.eGFP-Cre.WPRE.SV40). Four weeks after AAV2rg injection, male Rpl22-HA/AAV2rg-Cre+ were subjected to repeated social defeat (Stress) or left undisturbed (Con). Fourteen hours after repeated social defeat, the brain was collected, amygdala (AMYG) was dissected, polysome-bound neuronal mRNA was immunoprecipitated, and RNA was sequenced (n = 4). **B)** MA plot of differentially expressed genes (DEGs) in the amygdala projection neurons. The black dots represent significant genes ($p < 0.05$). **C)** Volcano plot of differentially expressed genes in stress influenced neurons that project into the hippocampus from the amygdala. The blue triangles represent genes that were significantly decreased with |log2FoldChange| >0. The red triangles represent genes that were significantly increased with |log2FoldChange| > 0. **D)** Ingenuity pathway analysis of canonical pathways of neurons that project into the hippocampus from the amygdala (|z-score| > 1.5). **E)** Ingenuity pathway analysis of canonical pathways inhibited by stress compared to control (|z-score| > 1.5). Number of DEGs associated with each pathway are represented in the bar corresponding to that pathway. **F)** Heat map of DEGs ($p < 0.05$) of neurons that project to the hippocampus from the amygdala associated synaptogenesis, CREB signaling, neuroinflammation, oxidative phosphorylation, nitric oxide (NO), reactive oxygen species (ROS) production, integrin signaling, and Rho GTPases signaling determined by Ingenuity Pathway Analysis. (For interpretation of the references to color in this figure legend, the reader is referred to the Web version of this article.)

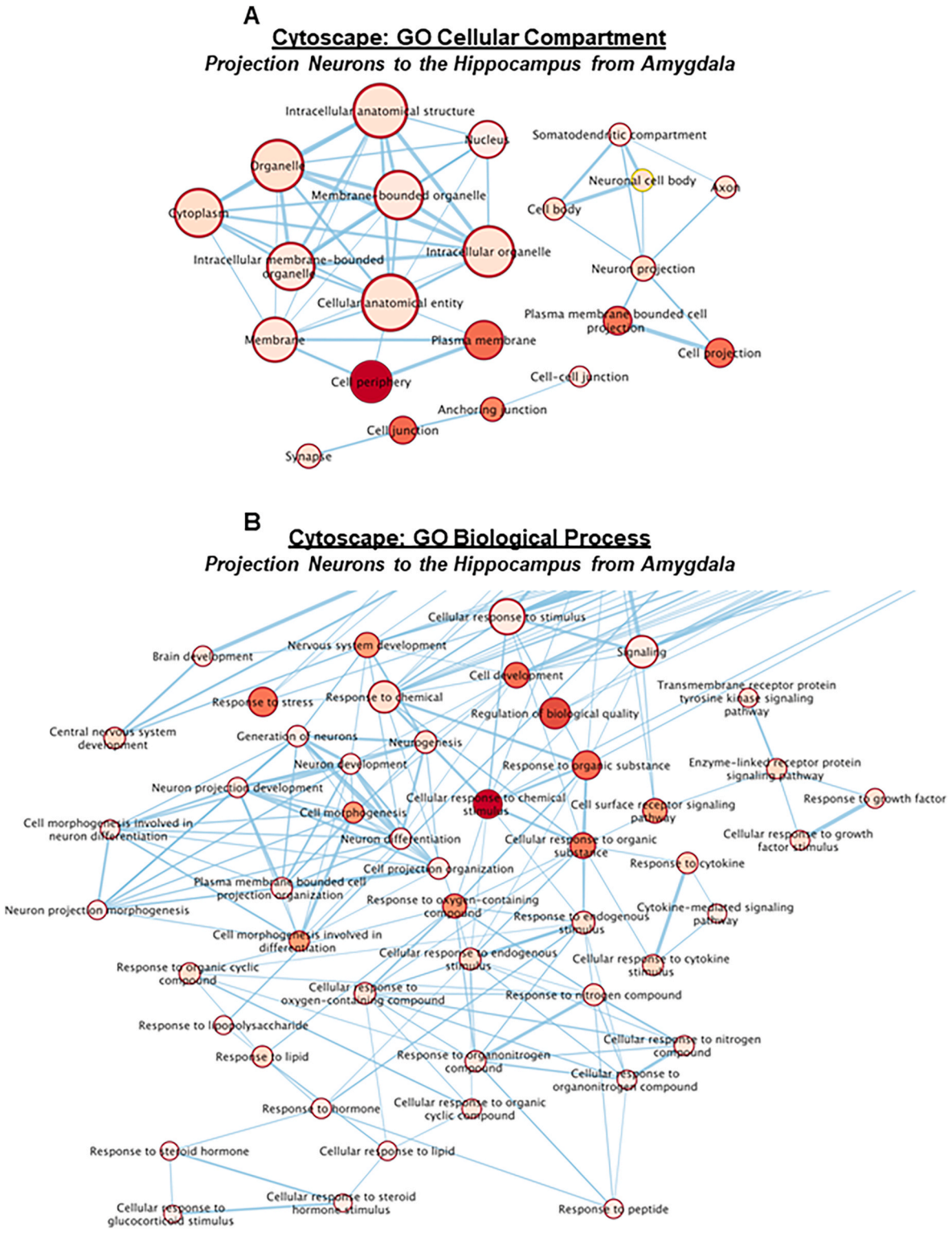

Fig. 6. Enrichment maps of cellular compartments and biological processes in amygdala projection neurons after Repeated Social Defeat. A) Gene Ontology Cellular Compartment determined by Cytoscape EnrichmentMap (CEM) that were affected in amygdala projection neurons after Stress. Circle size represents the number of genes within the category and the color of the circle represents the relative strength of connections. **B)** Gene Ontology Biological Process determined by Cytoscape EnrichmentMap (CEM) that affected in amygdala projection neurons after Stress. Circle size represents the number of genes within the category and the color of the circle represents the relative strength of connections. (For interpretation of the references to color in this figure legend, the reader is referred to the Web version of this article.)

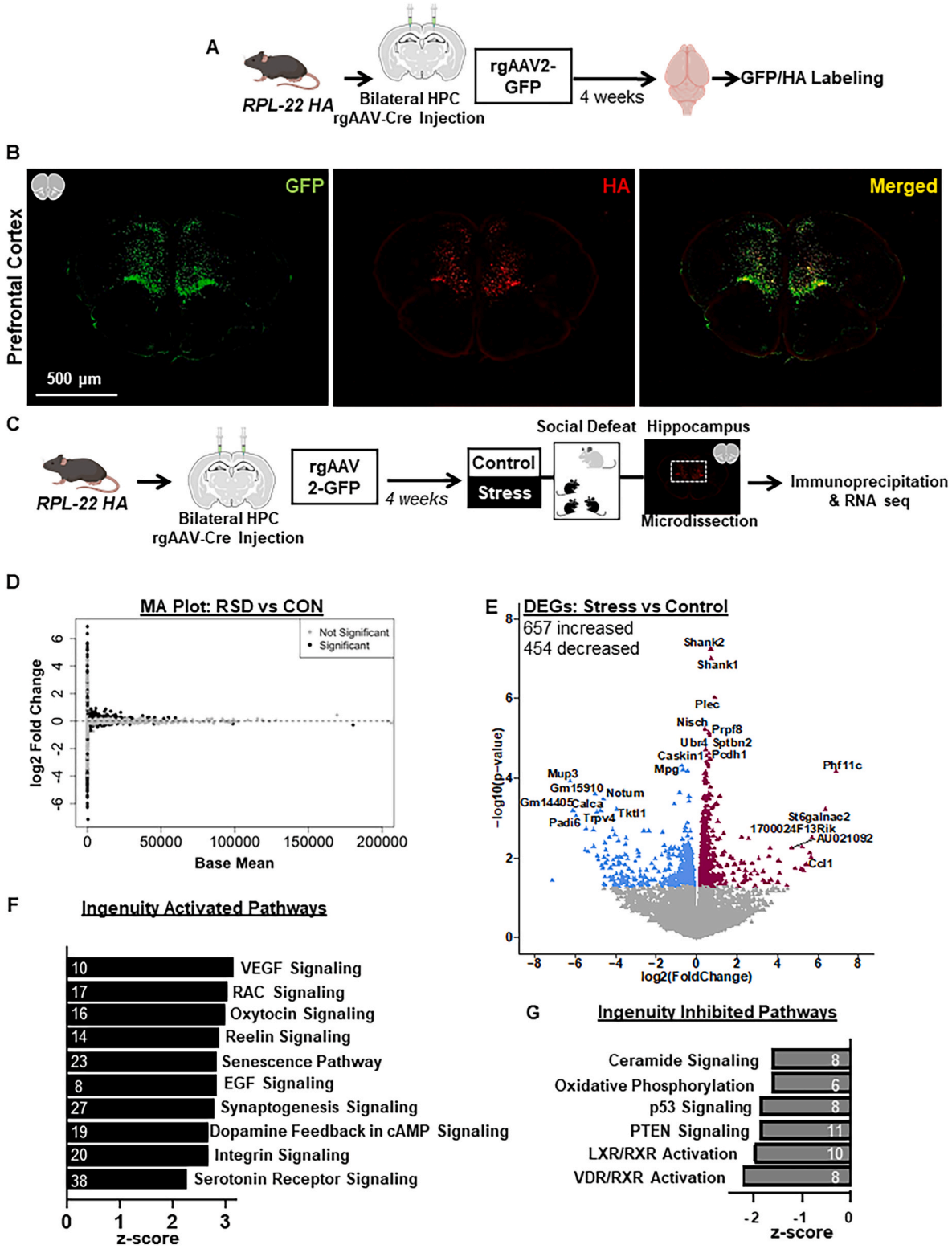

(caption on next page)

Fig. 7. Stress increased expression of genes associated with synaptogenesis, integrin signaling, and dopaminergic signaling in prefrontal cortical projection neurons. A) Diagram shows male RiboTag (Rpl22-HA) mice injected bilaterally into the CA1 region of the hippocampus (HPC) with a retrograde (rg) AAV2–Cre (pENN.AAV2rg.hSyn.HI.eGFP-Cre.WPRE.SV40). Brain sections were collected 4 weeks later and expression of AAV2rg and HA were determined (n = 5). **B)** Representative images of AAV2rg (green), HA (red), and co-localization (yellow) labeling in a prefrontal cortex (tile scan, 4x) of AAV2rg-RiboTag mice. **C)** Diagram shows male RiboTag (Rpl22-HA) mice injected bilaterally into the CA1 region of the hippocampus (HPC) with a retrograde AAV2–Cre (pENN.AAV2rg.hSyn.HI.eGFP-Cre.WPRE.SV40). Four weeks after AAV2rg injection, male Rpl22-HA/AAV2rg-Cre + mice were subjected to repeated social defeat (Stress) or left undisturbed (Con). Fourteen hours after repeated social defeat, the brain was collected, prefrontal cortex (PFC) was dissected, polysome-bound neuronal mRNA was immunoprecipitated, and RNA was sequenced (n = 3–6). **D)** MA plot of differentially expressed genes (DEGs) in the prefrontal cortex projection neurons. The black dots represent significant genes ($p < 0.05$). **E)** Volcano plot of differentially expressed genes of neurons that project into the hippocampus from the prefrontal cortex (indirect). The blue triangles represent genes that were significantly decreased with |log2FoldChange| >0. The maroon triangles represent genes that were significantly increased with |log2FoldChange| > 0. **F)** Ingenuity pathway analysis of canonical pathways activated by stress compared to control (|z-score| > 1.5). Number of DEGs associated with each pathway are represented in the bar corresponding to that pathway. **G)** Ingenuity pathway analysis of canonical pathways inhibited by stress compared to control in the PFC (|z-score| > 1.5). (For interpretation of the references to color in this figure legend, the reader is referred to the Web version of this article.)

that project into the hippocampus from the amygdala ($p < 0.05$, Fig. 9B). There were 34 shared DEGs between these distinct projection neurons, with 28 shared common directionalities following RSD (20 increased, 8 decreased, Fig. 9B). Moreover, RSD had the opposite effect on 6 DEGs in these projection neurons (e.g., *Itga9, Trpv4, Tha1,* $p < 0.05$, Fig. 9C). Thus, there is a unique RNA profile in the projection neurons amygdala to the hippocampus and neurons in the prefrontal cortex after RSD.

Next, unique or overlapping canonical pathways were determined using IPA. There were 11 unique canonical pathways in the prefrontal cortex (Fig. 9D) after RSD including P2Y Purinergic Receptor Signaling, Serotonin Receptor Signaling, EGF Signaling, and JAK/STAT Signaling (Fig. 9F). There were no unique canonical pathways in the amygdala following RSD. There were 41 shared canonical pathways between the prefrontal cortex and the amygdala. For example, RSD activated IL-6 Signaling, Integrin Signaling, Neuroinflammation, Synaptogenesis Signaling and inhibited PTEN Signaling and LXR/RXR activation in both the prefrontal cortex and amygdala projection neurons (Fig. 9E). Additionally, unique or overlapping master regulators were assessed. There were 4 master regulators that were unique to prefrontal cortex (e.g., Psen2, Il-4r), 10 master regulators that were unique to amygdala (e.g., Il-1β, S1pr4, Irf8), and 1 shared (Ifng, Fig. 9G and H). Taken together, neurons projecting from the amygdala to the hippocampus and neurons projecting from the prefrontal cortex have both unique and shared responses to RSD.

Comparison of hippocampal neurons, cortical projection neurons, amygdala projection neurons after Repeated Social Defeat. Building on the previous approach, we aimed to further investigate regional differences in the brain after RSD. The RNA sequencing datasets for the hippocampal neurons, neurons that project into the hippocampus (Figss. 2–3) from the amygdala (Figss. 5–6) and projection neurons from the prefrontal cortex (Figss. 7–8) were compared. The first stratified Rank-Rank Plot shows overlap in the concordant quadrants (i.e. genes upregulated and downregulated in both regions) in the amygdala and hippocampus after Stress (Fig. 10A). The second stratified Rank-Rank Plot shows overlap in the discordant quadrants (e.g. genes upregulated in hippocampus and downregulated in prefrontal cortex) and overlap in genes downregulated in the hippocampus and prefrontal cortex after Stress (Fig. 10A). The Venn diagram in Fig. 10B shows unique and shared DEGs in hippocampal neurons, projection neurons from amygdala to the hippocampus, and projection neurons from the prefrontal cortex. For instance, hippocampal neurons had 1436 unique DEGs compared to 952 unique DEGs in prefrontal cortex projection neurons and 525 unique DEGs in amygdala projection neurons after RSD ($p < 0.05$, Fig. 10B). There were 3 shared DEGs (*Anxa3, Ints8, Sgk1*, Fig. 10B). Thus, there is a unique RNA profile in hippocampal neurons, amygdala projection neurons to the hippocampus, and projection neurons in the prefrontal cortex after RSD.

Next, unique or overlapping canonical pathways were determined using IPA. NRF2-mediated Oxidative Stress Response was the only unique canonical pathway in the hippocampus (Fig. 10C and D). There were 6 unique canonical pathways in the prefrontal cortex (Fig. 10C and D) after RSD including Serotonin Receptor Signaling (Fig. 10C and D). There were no unique canonical pathways in the amygdala following RSD. There were 55 shared canonical pathways between the hippocampus, prefrontal cortex, and the amygdala. For example, RSD activated IL-6 Signaling, Integrin Signaling, Reelin Signaling, VEGF Signaling, Neuroinflammation, and inhibited PTEN Signaling and Endocannabinoid cancer inhibition pathway activation in both the prefrontal cortex and amygdala projection neurons (Fig. 10E). Additionally, unique or overlapping master regulators were assessed. There were 5 master regulators unique to the hippocampus (e.g., PSEN1, DRD2), 3 master regulators that were unique to prefrontal cortex (e.g., MTOR, IL4R), and 8 master regulators that were unique to amygdala (e.g., Il-1β, S1pr4, Irf8, Fig. 10F and G). There were no shared master regulators between all three regions. Taken together, hippocampal neurons, projection neurons from the amygdala to the hippocampus, and prefrontal cortex projection neurons have both unique and shared responses to RSD.

4. Discussion

In the current study, we sought to determine the stress-induced transcriptional signature of neurons within the hippocampus, projection neurons in the prefrontal cortex, and neurons that project from the amygdala. We aimed to increase our understanding of pathways and gene expression that was enhanced in neurons after social defeat that may underlie stress sensitization (Biltz et al., 2022). RiboTag mouse lines and retrograde AAV2-Cre approaches were used in male mice to tag, trace, and capture neurons influenced by stress in selected brain regions. In the hippocampus, there were 1632 DEGs after RSD associated with increase oxidative stress, synaptic long-term potentiation, and neuroinflammatory signaling. Prefrontal cortical projection neurons had RNA profiles associated with increased synaptogenesis, integrin signaling, and dopamine feedback signaling after RSD. Amygdala neurons that project into the hippocampus had RNA profiles associated with increased synaptogenesis, neuroinflammation signaling (e.g., IL-1 signaling), and NO and ROS production. Aspects of the stress response were shared between the neurons that project into the hippocampus and other pathways were region dependent. These data show unique RNA profiles of projection neurons and were associated with hippocampal dependent behavioral and cognitive deficits after RSD.

One relevant finding was that RSD-induced anxiety-like behavior in the EPM and increased spatial memory deficits in novel object location testing. The anxiety in the EPM data are consistent with previous studies showing that RSD caused anxiety-like behavior in the open field, light/dark preference and social avoidance tests (McKim et al., 2018; Wohleb et al., 2011, 2013). The insight here is that the EPM is an amygdala-hippocampal related task (Walf and Frye, 2007). This study represents the first time that we evaluated EPM testing after RSD. Moreover, another version of social defeat, 30 days of 5 min defeat stress, showed anxiety-like behavior in the EPM task (Jianhua et al.,

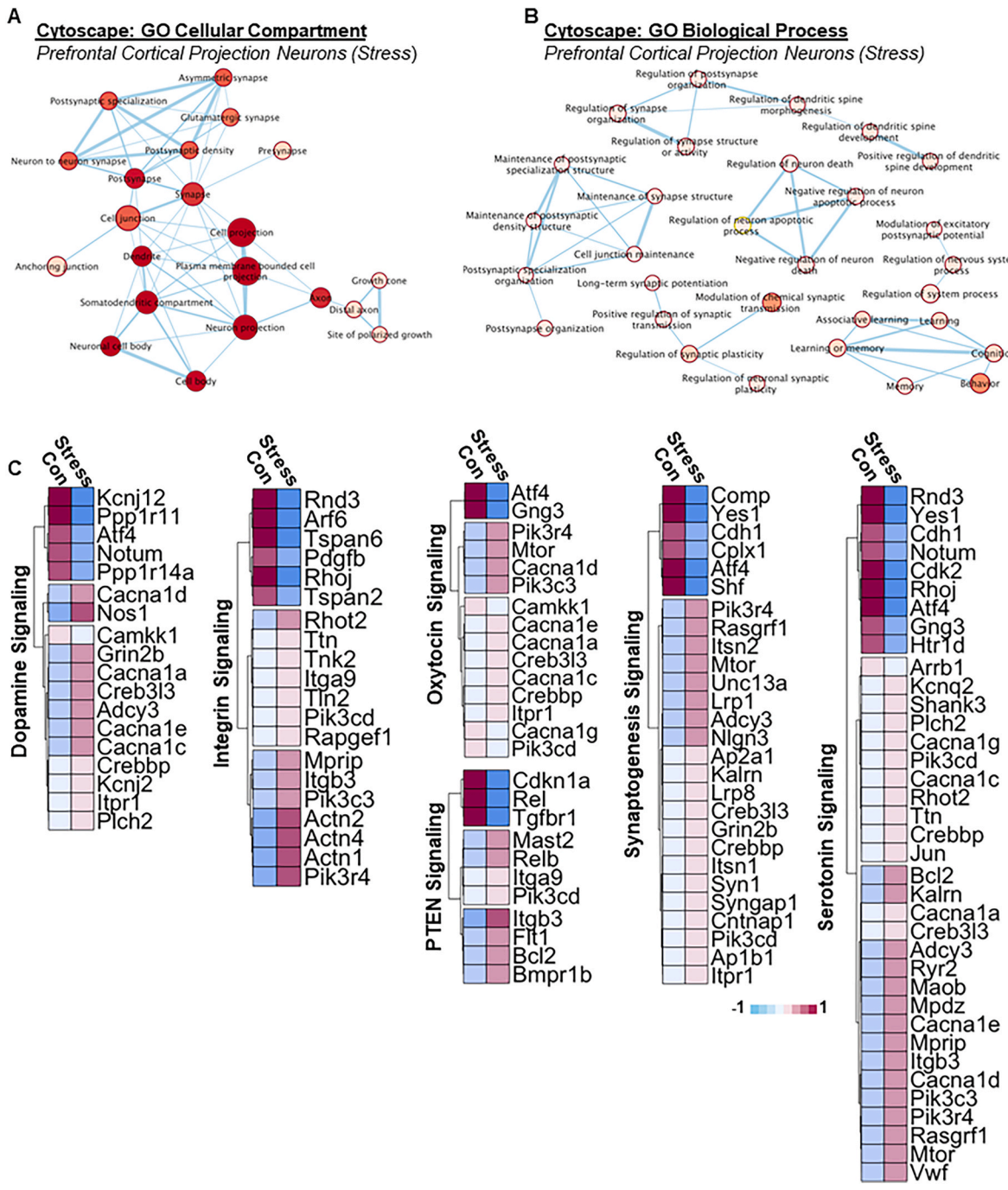

Fig. 8. Enrichment maps of cellular compartments and biological processes in prefrontal cortex projection neurons after Repeated Social Defeat. A) Gene Ontology Cellular Compartment determined by Cytoscape EnrichmentMap (CEM) that were affected in prefrontal cortex projection neurons after Stress. Circle size represents the number of genes within the category and the color of the circle represents the relative strength of connections. **B)** Gene Ontology Biological Process determined by Cytoscape EnrichmentMap (CEM) that affected in prefrontal cortex projection neurons after Stress. Circle size represents the number of genes within the category and the color of the circle represents the relative strength of connections. **C)** Heat map of DEGs ($p < 0.05$) of prefrontal cortex projection neurons associated with dopamine signaling, integrin signaling, oxytocin signaling, PTEN signaling, synaptogenesis signaling, and serotonin signaling determined by Ingenuity Pathway Analysis. (For interpretation of the references to color in this figure legend, the reader is referred to the Web version of this article.)

2017). NOR/NOL testing assesses cortical-hippocampal and amygdala-hippocampal memory (Barsegyan et al., 2014; Denninger et al., 2018). Deficits in this task are linked to brain regions affected by stress including the hippocampus (Barker and Warburton, 2011; de Lima et al., 2006), prefrontal cortex (Barker and Warburton, 2011), and amygdala (Zhao et al., 2021). Other stressors caused deficits in NOR/-NOL. For instance, mice exposed to a similar paradigm of social defeat stress (SDS) spent less time with the novel object compared to the familiar object (Zhao et al., 2021). This decrease in object recognition corresponded with a decrease in dopamine receptor-1 (D1) in the amygdala. Moreover, rats did not recognize the novel location when subjected to a bilateral dorsal hippocampus lesion (Barker and Warburton, 2011). In another experiment, when the connection between the medial prefrontal cortex and hippocampus was disrupted, rats had no deficits in novel object recognition or location, but instead had deficits in object-in-place recognition memory (Barker and Warburton, 2011).

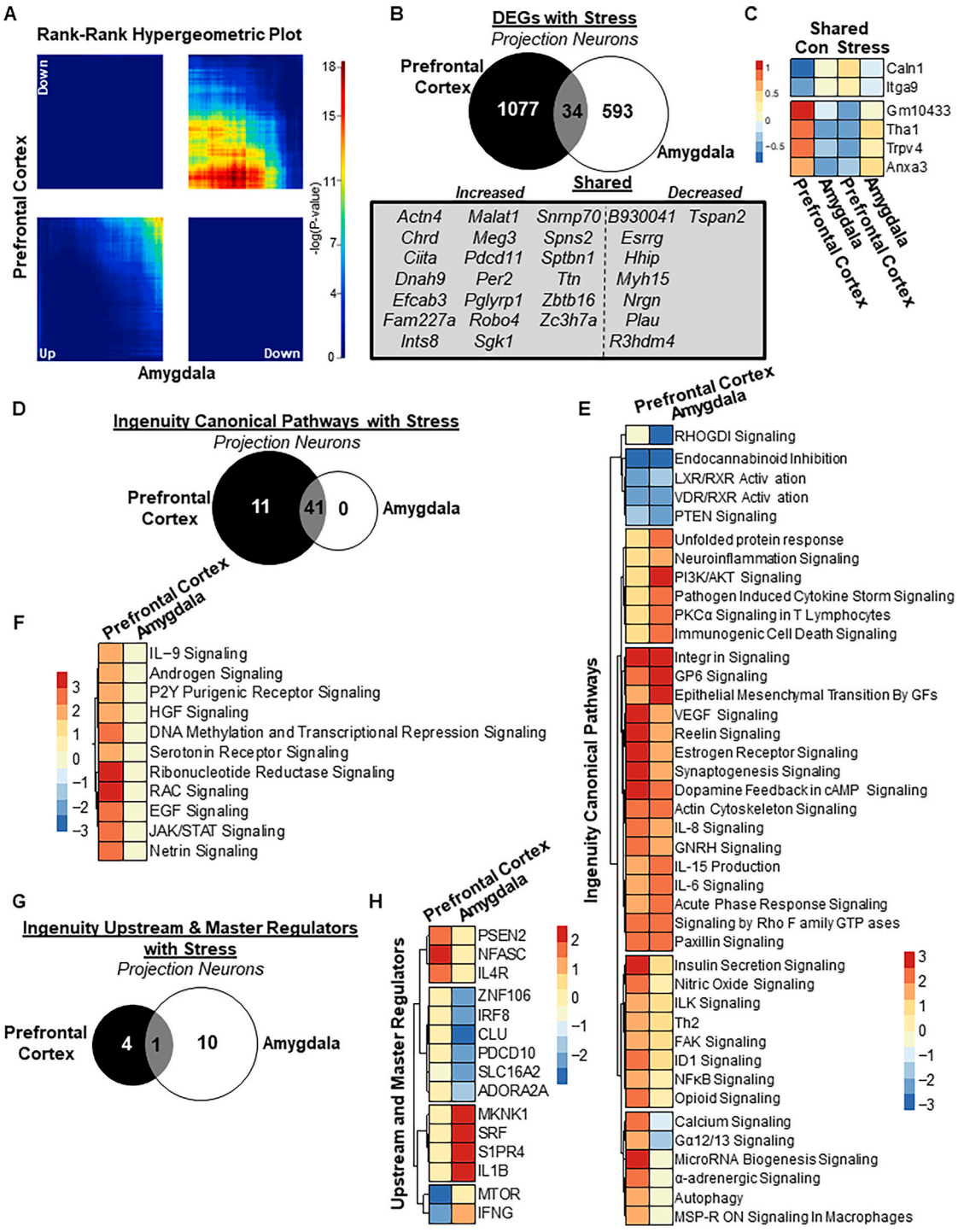

Fig. 9. Comparison of cortical and amygdala projection neurons after Repeated Social Defeat. The Rpl22-HA/AAV2rg-Cre bulk RNAseq data from amygdala (Figss. 5–6) and prefrontal cortex (Figss. 7–8) projection neurons after Stress. **A)** Heatmap of a Rank-Rank Hypergeometric plot comparing differentially expressed genes in the prefrontal cortex and amygdala. The bottom left quadrant represents genes upregulated in both regions, while the top right quadrant represents genes downregulated in both regions. The top left and bottom right quadrants depict genes that exhibit opposite directions of regulation between the two regions. **B)** Venn diagram depicts the number of differentially expressed genes of projection neurons from the prefrontal cortex (black) and amygdala (white), and differentially expressed genes (DEGs) that were shared between regions (grey, $p < 0.05$). A list of shared DEGs that were either increased or decreased is provided. **C)** Heat map of differentially expressed genes ($p < 0.05$) of projection neurons from the prefrontal cortex and amygdala. These are DEGs that are shared but moved in opposite directions in terms of expression. **D)** Venn diagram depicts canonical pathways (IPA) of projection neurons in the prefrontal cortex (black) and amygdala (white), and differentially expressed genes (DEGs) that were shared between regions (grey, $p < 0.05$). **E)** Heat map of canonical pathways that were shared between projection neurons in the prefrontal cortex and amygdala. Shades of red are increased pathways and shades of blue are decreased pathways. **F)** Heat map of canonical pathways that are uniquely increased in prefrontal cortex projection neurons compared to the amygdala. **G)** Venn diagram depicts upstream and master regulator (IPA) of neurons that project from the prefrontal cortex (black) and amygdala (white), and differentially expressed genes that were shared between regions (grey, $p < 0.05$). **H)** Heatmap of upstream and master regulators of projection neurons from the prefrontal cortex and amygdala. Shades of red are stress increased pathways and shades of blue are stress decreased pathways between these regions. (For interpretation of the references to color in this figure legend, the reader is referred to the Web version of this article.)

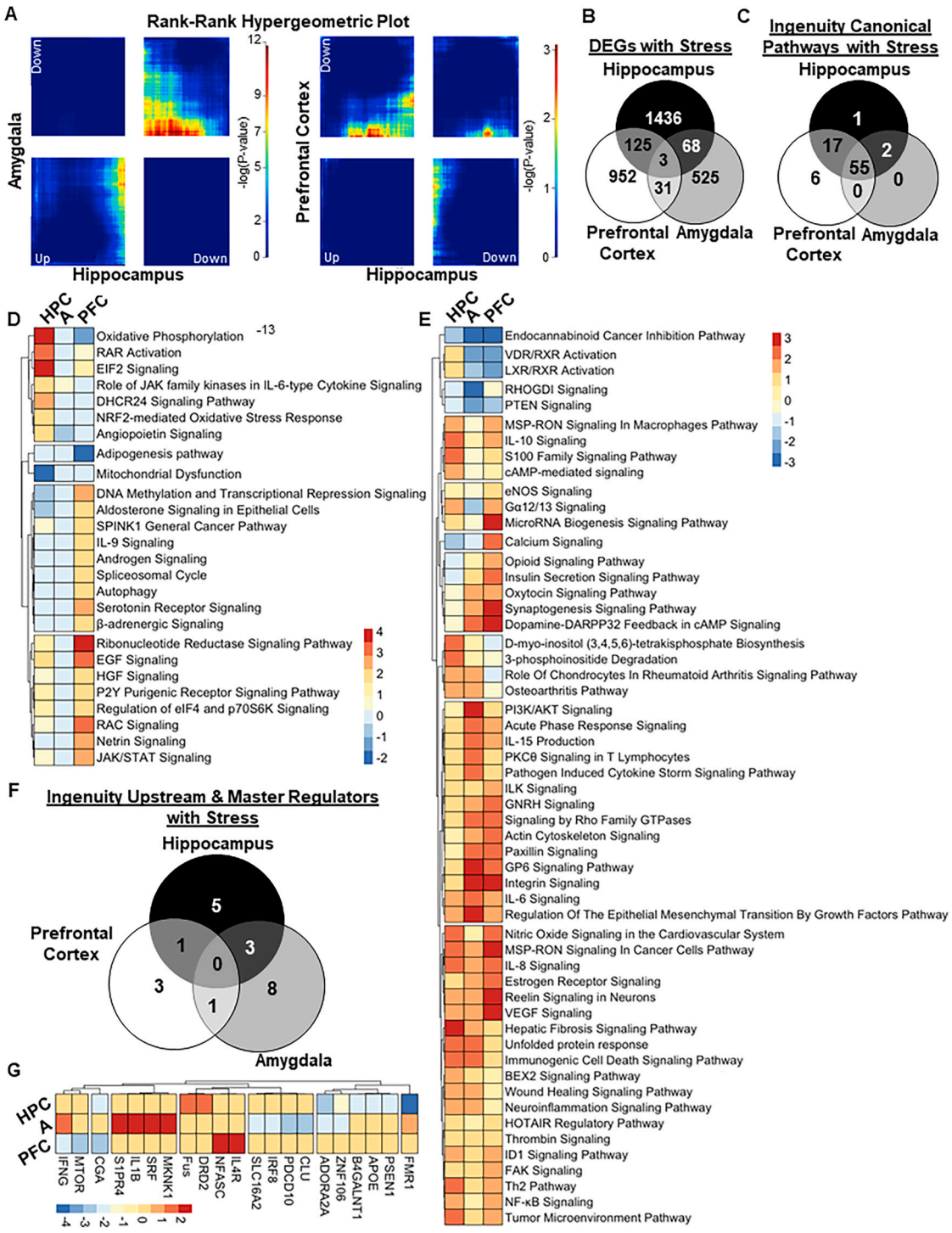

Fig. 10. Comparison of hippocampal neurons, cortical projection neurons, and amygdala projection neurons after Repeated Social Defeat. The Baf53b/Rpl22-HA bulk RNAseq data from the hippocampus (Figss. 2–3) and the Rpl22-HA/AAV2rg-Cre bulk RNAseq data from amygdala (Figss. 5–6) and prefrontal cortex (Figss. 7–8) projection neurons after Stress. **A)** Heatmap of a Rank-Rank Hypergeometric plot comparing differentially expressed genes in the prefrontal cortex and amygdala. The bottom left quadrant represents genes upregulated in both regions, while the top right quadrant represents genes downregulated in both regions. The top left and bottom right quadrants depict genes that exhibit opposite directions of regulation between the two regions. **B)** Venn diagram depicts canonical pathways (IPA) of hippocampal neurons (black), projection neurons in the prefrontal cortex (white) and amygdala (light grey), and differentially expressed genes (DEGs) that were shared between regions ($p < 0.05$). **C)** Venn diagram depicts canonical pathways (IPA) of hippocampal neurons (black), projection neurons in the prefrontal cortex (white) and amygdala (light grey), and differentially expressed genes (DEGs) that were shared between regions ($p < 0.05$). **D)** Heat map of canonical pathways that are uniquely influenced in one or two regions. **E)** Heat map of canonical pathways that were shared between hippocampal neurons and projection neurons in the prefrontal cortex and amygdala. Shades of red are increased pathways and shades of blue are decreased pathways. **F)** Venn diagram depicts upstream and master regulator (IPA) of hippocampal neurons (black), projection neurons in the prefrontal cortex (white) and amygdala (light grey), and differentially expressed genes (DEGs) that were shared between regions ($p < 0.05$). **G)** Heatmap of upstream and master regulators of hippocampal neurons and projection neurons from the prefrontal cortex and amygdala. Shades of red are stress increased pathways and shades of blue are stress decreased pathways between these regions. (For interpretation of the references to color in this figure legend, the reader is referred to the Web version of this article.)

This is relevant because it highlights the connection between the prefrontal cortex and the hippocampus in the context of memory formation and consolidation. Overall, repeated social defeat in male mice increased hippocampal-associated behavioral and memory deficits.

In this study, RNA profiles of hippocampal neurons were determined after RSD Activation of neurons in the hippocampus (cfos, FosB) was evident after RSD and noradrenergic dependent (Ramirez et al., 2015; Ramirez and Sheridan, 2016; Wohleb et al., 2011). Here, we captured the active RNA in neurons of the hippocampus after RSD using Pan-neuronal Ribotag mice (Baf53b/Rpl22-HA). In the hippocampus, RSD increased canonical pathways in neurons consistent with neuronal activation and reactivity including Gαs Signaling, Reeling Signaling, and cAMP Signaling. This was consistent with DEGs that are associated with glutamatergic signaling, memory formation and consolidation, and synaptic plasticity. For instance, RSD decreased calcium/calmodulin-dependent protein kinase IV (Camk4) and Regulator of G Protein Signaling 14 (Rgs14) and increased Cholinergic Receptor Muscarinic 5 (Chrm5), Glutamate Metabotropic Receptor 2 (Grm2), and Adrenoceptor Alpha 2C (Adra2c) in the hippocampus. These data are relevant because dysregulated glutamatergic signaling contributes to stress-related mood disorders like anxiety, depression, and PTSD in humans (Nishi et al., 2015; Sanacora et al., 2012). For example, glutamate levels in the serum were higher in individuals with PTSD compared to controls (Nishi et al., 2015). Individuals with higher glutamate levels in the serum had increased severity of PTSD. This idea is supported in rodent modeling of chronic stress (Highland et al., 2019; Schwendt and Jezova, 2000). For instance, Grm2 knock out in mice prevented the increase in immobility time during forced swim test and inescapable shock induced deficits after chronic social defeat stress (Highland et al., 2019). Thus, Grm2 is involved in stress-induced depressive-like behavior. It is possible that Grm2 is a key factor in neuronal sensitization and increased susceptibility for anxiety. Altogether, RSD increased genes associated with excitatory and glutamatergic signaling in the hippocampus.

A limitation of the pan-neuronal RiboTag (Baf53b/Rpl22-HA) approach was that the neuronal profile was unspecific to a type of neuron in the hippocampus. The hippocampus is enriched with neurons that are primarily glutamatergic excitatory neurons (~90%), while a small subset are inhibitory, GABAergic interneurons (Briend et al., 2020). Additionally, pathway analyses reveal that the neuronal genes changes were associated with increased glutamatergic and serotonergic signaling in the hippocampus. We interpret these data to indicate that neuronal gene changes in the hippocampus were associated with excitatory neuron signaling and were mediated through glutamatergic or serotonergic neurons after RSD. As such, our recent single nuclei RNAseq analysis showed that RSD increased glutamate and CREB signaling, BDNF, synaptic organization and cell morphogenesis in excitatory neurons of the dentate gyrus and CA1 of the hippocampus (Goodman et al., 2024). These data, especially evidence of enhanced plasticity, are consistent with the data from the pan-neuronal RiboTag approach. Overall, the general RNA profile of these RSD activated neurons of the hippocampus were associated with increased oxidative stress and metabolism, synaptic long-term potentiation, and neuroinflammatory signaling.

A novel approach of this study was using RiboTag mice and retrograde-adeno-associated-virus-2 to trace and capture HA-tagged neurons that project into the hippocampus. Here a retrograde-adeno-associated-virus (AAV2rg) expressing Cre-recombinase was injected into the dorsal hippocampus of RiboTag mice. This induced an expression of a hemagglutinin-epitope (HA) tag within neurons that projected into the hippocampus. This is relevant because the dorsal hippocampus is involved in the interpretation of stimuli related to fear and threat. Ribosomal bound mRNA, which represents mRNA that is actively being translated into protein, was collected after social defeat for RNA-sequencing from the amygdala and prefrontal cortex. We show that the AAV2rg injection into the CA1 spreads throughout the hippocampus (including the dentate gyrus) and out to other projection neurons from amygdala, detected by labeling of both GFP and HA. The connections from the prefrontal cortex to the hippocampus are reported to be indirect and are relayed through other brain regions including the thalamic reunions (Dolleman-van der Weel et al., 2019). The AAV2rg-Cre virus used here, however, is monosynaptic. Thus, the HA-tagged neurons in the prefrontal cortex after AAV2rg injection into the hippocampus likely represents direct projections into the hippocampus. This circuit has not been established previously in rodents and more work is needed to prove this hypothesis. Another possibility is that some AAV2rg-Cre leaked in the cortex during hippocampal injection. If so, this would capture prefrontal neurons that project within the cortex. Either way, these HA tagged neurons represent project neurons from the prefrontal cortex. Again, these HA-tagged neurons, co-expressing AAV2rg were evident in the prefrontal cortex after AAV2rg-Cre injection into the CA1. In addition, the HA-tagged neurons in the basolateral amygdala that project to the hippocampus did not co-express parvalbumin (PV). PV^{+} neurons comprise 50% of the inhibitory interneuron population in the BLA (Babaev et al., 2018). The BLA is comprised mostly of excitatory neurons. Thus, these connections are likely excitatory. This is consistent with previous findings that the basolateral amygdala is highly enriched with glutamatergic pyramidal neurons (Pape and Pare, 2010; Sah et al., 2003). Therefore, we interpret these data to indicate that these projection neurons activated after RSD in the amygdala and project to the hippocampus are excitatory.

Another relevant finding was that the prefrontal cortex projection neurons that had RNA profiles associated with increased Synaptogenesis, Integrin Signaling, Reelin Signaling, Serotonin Signaling and Dopamine Feedback in cAMP Signaling after RSD. Of interest, synaptogenesis and reelin signaling were increased after RSD in prefrontal cortex projection neurons. The current study represents cortical RNA changes after repeated social defeat. For instance, reelin signaling is associated with synaptogenesis, dendritic spine formation, and plasticity (Ishii et al., 2016; Wasser and Herz, 2017). Specifically, increased RNA and protein levels of reelin in the medial prefrontal cortex correlated with long-term potentiation inductions (Sui et al., 2012). Notably, other rodent studies of chronic stress reported reduced expression of reelin, which is consistent with the development of depressive-like behavior in rats that received repeated injections of corticosterone (CORT) (Lebedeva et al., 2020). In addition, reduced reelin is linked to other neuropsychiatric diseases in humans including schizophrenia (Impagnatiello et al., 1998). Indeed, over expression of reelin in the brain reduced time spent floating in the forced swim test (depressive-like behavioral task) and reduced pre-pulse inhibition (schizophrenia-like behavioral task) (Teixeira et al., 2011). Nonetheless, reelin signaling and synaptogenesis were enhanced in these cortical projection neurons after RSD. We predict that these increases in reelin and synaptogenesis enhance neuronal plasticity. Enhanced plasticity after RSD is consistent with increased fear memory (Goodman et al., 2024; Lisboa et al., 2018) and increased neuronal reactivity to subthreshold stressors after RSD (Lisboa et al., 2018; Weber et al., 2019; Wohleb et al., 2014a). Therefore, Reelin signaling is a relevant pathway in the stress sensitivity of neurons and may contribute to increased plasticity after stress.

Similar to the RNA profiles of other fear and threat appraisal regions, amygdala neurons that project into the hippocampus had RNA profiles associated with increased synaptogenesis, neuroinflammatory signaling (e.g., IL-1 signaling), and NO and ROS production. Notably, there were 12 DEG's associated with glutamatergic and excitatory signaling in the amygdala. For example, RSD increased metabotropic glutamate receptor 2 (*Grm2*) and Inositol 1,4,5-Trisphosphate Receptor-3 (*Itpr3*) and decreased leucine rich repeat transmembrane neuronal 2 (*Lrrtm2*), Cannabinoid Receptor 1 (*Cnr1*) and Glycogen Synthase Kinase 3 Beta (*Gsk3b*). Again, these genes/pathways are relevant to neuronal homeostasis and plasticity. For instance, Lrrtm2 knock out in mice caused impaired neuronal function and LTP (Bhouri et al., 2018). Moreover, when excitatory (glutamatergic) projection neurons from the amygdala

(BLA) to the hippocampus were inhibited, there was a decrease in anxiety-like behavior (Felix-Ortiz et al., 2013). These findings highlight that the circuit from the amygdala to the hippocampus contributes to the development of anxiety-like behavior. Furthermore, our previous work shows that neuronal reactivity ($pCREB^+$) is increased in stress responsive regions (e.g., hippocampus, prefrontal cortex) after an acute stress exposure 24 days after RSD (Weber et al., 2019). Here, we show that *Camk2d* (Calcium/calmodulin-dependent protein kinase type II subunit delta) and *Vegfa* (vascular endothelial growth factor A) are associated with CREB signaling and were increased after RSD. Therefore, it is possible that these two genes play a role in stress re-exposure or sensitization. Another point of interest is the increase in neuroinflammation signaling, specifically IL-1 signaling in the amygdala projection neurons after RSD. IL-1R1 expression on glutamatergic neurons in the hippocampus was critical in the development of anxiety-like behavior and cognitive deficits after RSD (DiSabato et al., 2021). IL-1R1 knockout on glutamatergic neurons prevented social defeat-induced anxiety-like behavior, impairments in social interaction, and working memory deficits (DiSabato et al., 2021). When IL-1R1 was restored on glutamatergic neurons there was a re-establishment of anxiety and social interaction deficits (DiSabato et al., 2021). Furthermore, RSD-mice re-exposed to an acute stressor 24 days later had an increase in neuronal reactivity ($pCREB^+$) in the hippocampus, social withdrawal, and working memory deficits and this was prevented with the IL-1R1 knockout on glutamatergic neurons (DiSabato et al., 2022). Parallel to this, IL-1R1 is increased activated neurons that project from the amygdala to the hippocampus after RSD. Altogether, glutamatergic signaling and IL-1 signaling from the amygdala to the hippocampus likely contributes to both the development of anxiety-like behavior and neuronal sensitization after RSD.

Another point of interest was the comparison of the two data RNAseq data sets of stress influenced neurons that project into the hippocampus from the amygdala and projection neurons from the prefrontal cortex. Coinciding with the hippocampus, these regions are also critical to the response to stress and contribute to fear memory and anxiety-like behaviors (Lisboa et al., 2018; McKim et al., 2018). In projection neurons from the prefrontal cortex, there were 11 unique pathways including IL-9 Signaling, Purinergic Signaling, and Serotonin Receptor. There were 41 shared canonical pathways between the prefrontal cortex and amygdala after RSD. This included an increase in integrin signaling, synaptogenesis signaling, reelin signaling, dopamine feedback, actin cytoskeleton signaling, IL -6, IL -15, and neuroinflammatory signaling. There were decreases in RXR activation and PTEN signaling. Stress increased calcium signaling and Gα12/13 signaling in the prefrontal cortex while it was decreased in the amygdala neurons that project to the hippocampus. In conclusion, the analysis of RNAseq data from neurons projecting to the hippocampus from the amygdala and projection neurons from the prefrontal cortex revealed distinct and shared pathways, shedding light on the response to stress and its role in regulating fear memory and anxiety-like behavior in these critical brain regions.

Although the amygdala did not have any unique canonical pathways after stress, there were myriad DEGs and 10 upstream regulators that were unique to the amygdala. For instance, increased upstream regulators, IL-1β and Sphingosine 1-phosphate (S1PR1), were unique to the neurons from the amygdala that project into the hippocampus. The pro-inflammatory cytokine, IL-1β is of particular importance because the DG of the hippocampus has robust expression of the IL-1 receptor-1 (IL-1R1). Previous reports indicated that IL-1R1 on glutamatergic neurons is involved with the sensitization of neurons (increased $pCREB^+$ reactivity) after RSD (DiSabato et al., 2022). For example, mice that were exposed to RSD then exposed to an acute defeat (1 cycle of RSD) at day30 had increased neuronal reactivity (pCREB) and neuronal activation (fosb) in the hippocampus. This was prevented with the neuronal IL-1R1 knockout on glutamatergic neurons (DiSabato et al., 2022). Additionally, the main sources of IL-1β production and release are predicted to be from myeloid cells, microglia and monocyte (McKim et al., 2018), but an interpretation of these data is that there is a neuronal source of IL-1β. Moreover, this might be a neuronal signal that integrates in the DG of the hippocampus from other brain regions including the amygdala to influence behavior. This idea is further supported by our recent study showing that RSD increased contextual fear memory that was dependent on IL-1 receptor-1 in excitatory neurons ($Vglut2^+$ neurons in the DG) but independent of microglia (Goodman et al., 2024). An additional inflammatory component is the upstream regulator S1PR1. S1PR1 is associated with the trafficking of leukocytes (Massberg et al., 2007), vascular integrity (Akhter et al., 2021), and neuronal excitability (Mork et al., 2022). Inflammatory monocytes are actively recruited to the brain after RSD by microglia. These monocytes interact with endothelia and cause prolonged anxiety-like behavior (McKim et al., 2018; Wohleb et al., 2013, 2014b; Yin et al., 2022). Furthermore, S1PR1 can increase the release of ATP which can bind onto purinergic receptors (e.g., P2X7). This is relevant because purinergic receptor activation on microglia via P2X7 leads to increased IL-1β. This pathway is implicated in stress-related mood disorders in humans. In RSD, there is evidence that a P2X7 antagonist prevented stress-induced microglia reactivity, IL-1β RNA in microglia, and the development of anxiety-like behavior (Biltz et al., 2024). Thus, S1PR1 in neurons in the amygdala may propagate microglia activation and the active recruitment of monocytes after RSD within this region. Therefore, these region selective responses in the brain are important for understanding the differential signaling that occurs with fear and threat appraisal.

A limitation of the current study is that only male mice were used. Previous studies have established that social defeat in females is possible but requires the use of a modified social defeat paradigm with male DREADD aggressors (Dion-Albert et al., 2022; Takahashi et al., 2017). Using this model, female mice have neuronal activation in stress responsive regions and anxiety-like behavior after social defeat (Yin et al., 2019). Thus, we predict that the neuronal profile in the hippocampus, prefrontal cortex, and amygdala would be similar in female mice exposed to modified social defeat. Nonetheless, these experiments need to be completed in females to confirm this hypothesis.

In conclusion, stress induced a unique pattern of gene expression within activated neurons that project into the hippocampus from the amygdala and projection neurons from the prefrontal cortex. These findings provide new insights into how the hippocampus integrates signaling from discrete brain areas after chronic stress. Moreover, we have new insights on pathways activated in neurons that may underlie stress sensitization after social defeat.

CRediT authorship contribution statement

Rebecca G. Biltz: Writing – review & editing, Writing – original draft, Visualization, Validation, Project administration, Methodology, Formal analysis, Data curation, Conceptualization. **Wenyuan Yin:** Writing – review & editing, Visualization, Methodology, Data curation, Conceptualization. **Ethan J. Goodman:** Writing – review & editing, Visualization, Methodology, Formal analysis, Data curation. **Lynde M. Wangler:** Writing – review & editing, Visualization, Project administration, Methodology, Formal analysis, Data curation. **Amara C. Davis:** Writing – review & editing, Visualization, Validation, Methodology, Formal analysis, Data curation. **Braedan T. Oliver:** Writing – review & editing, Validation, Methodology. **Jonathan P. Godbout:** Writing – review & editing, Writing – original draft, Visualization, Supervision, Resources, Methodology, Investigation, Funding acquisition, Conceptualization. **John F. Sheridan:** Writing – review & editing, Writing – original draft, Supervision, Resources, Investigation, Funding acquisition, Conceptualization.

Funding disclosure

The authors disclosed receipt of the following financial support for the research, authorship, and/or publication of this article: This research was supported by a NIMH R01 grant (MH-119670 to JFS & JG). RGB was supported by the Ohio State University Presidential Fellowship (to RGB). WY and LMW were supported by National Institute of Neurological Disorders and Stroke (NINDS) T32 grant (NS-105864). WY was also supported by a F30-MH-125524 (to WY).

Declaration of competing interest

There are no conflict of interest among all authors.

Acknowledgments

Elements of the figures, including schematics were created using Biorender.

Data availability

Data will be made available on request.

References

Akhter, M.Z., Chandra Joshi, J., Balaji Ragunathrao, V.A., Maienschein-Cline, M., Proia, R.L., Malik, A.B., Mehta, D., 2021. Programming to S1PR1(+) endothelial cells promotes restoration of vascular integrity. Circ. Res. 129, 221–236.

Babaev, O., Piletti Chatain, C., Krueger-Burg, D., 2018. Inhibition in the amygdala anxiety circuitry. Exp. Mol. Med. 50, 1–16.

Barker, G.R., Warburton, E.C., 2011. When is the hippocampus involved in recognition memory? J. Neurosci. 31, 10721–10731.

Barsegyan, A., McGaugh, J.L., Roozendaal, B., 2014. Noradrenergic activation of the basolateral amygdala modulates the consolidation of object-in-context recognition memory. Front. Behav. Neurosci. 8, 160.

Bhouri, M., Morishita, W., Temkin, P., Goswami, D., Kawabe, H., Brose, N., Sudhof, T.C., Craig, A.M., Siddiqui, T.J., Malenka, R., 2018. Deletion of LRRTM1 and LRRTM2 in adult mice impairs basal AMPA receptor transmission and LTP in hippocampal CA1 pyramidal neurons. Proc. Natl. Acad. Sci. U. S. A. 115, E5382–E5389.

Bijsterbosch, J., Smith, S., Bishop, S.J., 2015. Functional connectivity under anticipation of shock: correlates of trait anxious affect versus induced anxiety. J. Cognit. Neurosci. 27, 1840–1853.

Bilodeau, J., Schwendt, M., 2016. Post-cocaine changes in regulator of G-protein signaling (RGS) proteins in the dorsal striatum: relevance for cocaine-seeking and protein kinase C-mediated phosphorylation. Synapse 70, 432–440.

Biltz, R.G., Sawicki, C.M., Sheridan, J.F., Godbout, J.P., 2022. The neuroimmunology of social-stress-induced sensitization. Nat. Immunol. 23, 1527–1535.

Biltz, R.G., Swanson, S.P., Draime, N., Davis, A.C., Yin, W., Goodman, E.J., Gallagher, N. R., Bhattacharya, A., Sheridan, J.F., Godbout, J.P., 2024. Antagonism of the brain P2X7 ion channel attenuates repeated social defeat induced microglia reactivity, monocyte recruitment and anxiety-like behavior in male mice. Brain Behav. Immun. 115, 356–373.

Bray, C.E., Witcher, K.G., Adekunle-Adegbite, D., Ouvina, M., Witzel, M., Hans, E., Tapp, Z.M., Packer, J., Goodman, E., Zhao, F., Chunchai, T., O'Neil, S., Chattipakorn, S.C., Sheridan, J., Kokiko-Cochran, O.N., Askwith, C., Godbout, J.P., 2022. Chronic cortical inflammation, cognitive impairment, and immune reactivity associated with diffuse brain injury are ameliorated by forced turnover of microglia. J. Neurosci. 42, 4215–4228.

Briend, F., Nelson, E.A., Maximo, O., Armstrong, W.P., Kraguljac, N.V., Lahti, A.C., 2020. Hippocampal glutamate and hippocampus subfield volumes in antipsychotic-naive first episode psychosis subjects and relationships to duration of untreated psychosis. Transl. Psychiatry 10, 137.

Cole, S.W., Arevalo, J.M., Takahashi, R., Sloan, E.K., Lutgendorf, S.K., Sood, A.K., Sheridan, J.F., Seeman, T.E., 2010. Computational identification of gene-social environment interaction at the human IL6 locus. Proc. Natl. Acad. Sci. U. S. A. 107, 5681–5686.

de Lima, M.N., Luft, T., Roesler, R., Schroder, N., 2006. Temporary inactivation reveals an essential role of the dorsal hippocampus in consolidation of object recognition memory. Neurosci. Lett. 405, 142–146.

Deji, C., Yan, P., Ji, Y., Yan, X., Feng, Y., Liu, J., Liu, Y., Wei, S., Zhu, Y., Lai, J., 2022. The basolateral amygdala to ventral Hippocampus circuit controls anxiety-like behaviors induced by morphine withdrawal. Front. Cell. Neurosci. 16, 894886.

Denninger, J.K., Smith, B.M., Kirby, E.D., 2018. Novel object recognition and object location behavioral testing in mice on a budget. J. Vis. Exp. 20 (141). https://doi.org/10.3791/58593.

Dion-Albert, L., Cadoret, A., Doney, E., Kaufmann, F.N., Dudek, K.A., Daigle, B., Parise, L. F., Cathomas, F., Samba, N., Hudson, N., Lebel, M., Signature, C., Campbell, M., Turecki, G., Mechawar, N., Menard, C., 2022. Vascular and blood-brain barrier-related changes underlie stress responses and resilience in female mice and depression in human tissue. Nat. Commun. 13, 164.

DiSabato, D.J., Nemeth, D.P., Liu, X., Witcher, K.G., O'Neil, S.M., Oliver, B., Bray, C.E., Sheridan, J.F., Godbout, J.P., Quan, N., 2021. Interleukin-1 receptor on hippocampal neurons drives social withdrawal and cognitive deficits after chronic social stress. Mol. Psychiatr. 26, 4770–4782.

DiSabato, D.J., Yin, W., Biltz, R.G., Gallagher, N.R., Oliver, B., Nemeth, D.P., Liu, X., Sheridan, J.F., Quan, N., Godbout, J.P., 2022. IL-1 Receptor-1 on Vglut2 (+) neurons in the hippocampus is critical for neuronal and behavioral sensitization after repeated social stress. Brain Behav Immun Health 26, 100547.

Dolleman-van der Weel, M.J., Griffin, A.L., Ito, H.T., Shapiro, M.L., Witter, M.P., Vertes, R.P., Allen, T.A., 2019. The nucleus reuniens of the thalamus sits at the nexus of a hippocampus and medial prefrontal cortex circuit enabling memory and behavior. Learn. Mem. 26, 191–205.

Felix-Ortiz, A.C., Beyeler, A., Seo, C., Leppla, C.A., Wildes, C.P., Tye, K.M., 2013. BLA to vHPC inputs modulate anxiety-related behaviors. Neuron 79, 658–664.

Goodman, E.J., Biltz, R.G., Packer, J.M., DiSabato, D.J., Swanson, S.P., Oliver, B., Quan, N., Sheridan, J.F., Godbout, J.P., 2024. Enhanced fear memory after social defeat in mice is dependent on interleukin-1 receptor signaling in glutamatergic neurons. Mol. Psychiatr. 29 (8), 2321–2334. Aug.

Goswamee, P., Leggett, E., McQuiston, A.R., 2021. Nucleus reuniens afferents in Hippocampus modulate CA1 network function via monosynaptic excitation and polysynaptic inhibition. Front. Cell. Neurosci. 15, 660897.

Hallock, H.L., Wang, A., Griffin, A.L., 2016. Ventral midline thalamus is critical for hippocampal-prefrontal synchrony and spatial working memory. J. Neurosci. 36, 8372–8389.

Harkness, K.L., Hayden, E.P., Lopez-Duran, N.L., 2015. Stress sensitivity and stress sensitization in psychopathology: an introduction to the special section. J. Abnorm. Psychol. 124, 1–3.

Highland, J.N., Zanos, P., Georgiou, P., Gould, T.D., 2019. Group II metabotropic glutamate receptor blockade promotes stress resilience in mice. Neuropsychopharmacology 44, 1788–1796.

Impagnatiello, F., Guidotti, A.R., Pesold, C., Dwivedi, Y., Caruncho, H., Pisu, M.G., Uzunov, D.P., Smalheiser, N.R., Davis, J.M., Pandey, G.N., Pappas, G.D., Tueting, P., Sharma, R.P., Costa, E., 1998. A decrease of reelin expression as a putative vulnerability factor in schizophrenia. Proc. Natl. Acad. Sci. U. S. A. 95, 15718–15723.

Ishii, K., Kubo, K.I., Nakajima, K., 2016. Reelin and neuropsychiatric disorders. Front. Cell. Neurosci. 10, 229.

Ito, H.T., Zhang, S.J., Witter, M.P., Moser, E.I., Moser, M.B., 2015. A prefrontal-thalamo-hippocampal circuit for goal-directed spatial navigation. Nature 522, 50–55.

Jianhua, F., Wei, W., Xiaomei, L., Shao-Hui, W., 2017. Chronic social defeat stress leads to changes of behaviour and memory-associated proteins of young mice. Behav. Brain Res. 316, 136–144.

Kiecolt-Glaser, J.K., Glaser, R., 2002. Depression and immune function: central pathways to morbidity and mortality. J. Psychosom. Res. 53, 873–876.

Kivinummi, T., Kaste, K., Rantamaki, T., Castren, E., Ahtee, L., 2011. Alterations in BDNF and phospho-CREB levels following chronic oral nicotine treatment and its withdrawal in dopaminergic brain areas of mice. Neurosci. Lett. 491, 108–112.

Lebedeva, K.A., Allen, J., Kulhawy, E.Y., Caruncho, H.J., Kalynchuk, L.E., 2020. Cyclical administration of corticosterone results in aggravation of depression-like behaviors and accompanying downregulations in reelin in an animal model of chronic stress relevant to human recurrent depression. Physiol. Behav. 224, 113070.

Lesting, J., Narayanan, R.T., Kluge, C., Sangha, S., Seidenbecher, T., Pape, H.C., 2011. Patterns of coupled theta activity in amygdala-hippocampal-prefrontal cortical circuits during fear extinction. PLoS One 6, e21714.

Lisboa, S.F., Niraula, A., Resstel, L.B., Guimaraes, F.S., Godbout, J.P., Sheridan, J.F., 2018. Repeated social defeat-induced neuroinflammation, anxiety-like behavior and resistance to fear extinction were attenuated by the cannabinoid receptor agonist WIN55,212-2. Neuropsychopharmacology 43, 1924–1933.

Mah, L., Szabuniewicz, C., Fiocco, A.J., 2016. Can anxiety damage the brain? Curr. Opin. Psychiatr. 29, 56–63.

Malivoire, B.L., Girard, T.A., Patel, R., Monson, C.M., 2018. Functional connectivity of hippocampal subregions in PTSD: relations with symptoms. BMC Psychiatr. 18, 129.

Martinez, M., Calvo-Torrent, A., Herbert, J., 2002. Mapping brain response to social stress in rodents with c-fos expression: a review. Stress 5, 3–13.

Massberg, S., Schaerli, P., Knezevic-Maramica, I., Kollnberger, M., Tubo, N., Moseman, E. A., Huff, I.V., Junt, T., Wagers, A.J., Mazo, I.B., von Andrian, U.H., 2007. Immunosurveillance by hematopoietic progenitor cells trafficking through blood, lymph, and peripheral tissues. Cell 131, 994–1008.

McEwen, B.S., 2013. The brain on stress: toward an integrative approach to brain, body, and behavior. Perspect. Psychol. Sci. 8, 673–675.

McKim, D.B., Niraula, A., Tarr, A.J., Wohleb, E.S., Sheridan, J.F., Godbout, J.P., 2016. Neuroinflammatory dynamics underlie memory impairments after repeated social defeat. J. Neurosci. 36, 2590–2604.

McKim, D.B., Weber, M.D., Niraula, A., Sawicki, C.M., Liu, X., Jarrett, B.L., Ramirez-Chan, K., Wang, Y., Roeth, R.M., Sucaldito, A.D., Sobol, C.G., Quan, N., Sheridan, J. F., Godbout, J.P., 2018. Microglial recruitment of IL-1beta-producing monocytes to brain endothelium causes stress-induced anxiety. Mol. Psychiatr. 23, 1421–1431.

Milad, M.R., Pitman, R.K., Ellis, C.B., Gold, A.L., Shin, L.M., Lasko, N.B., Zeidan, M.A., Handwerger, K., Orr, S.P., Rauch, S.L., 2009. Neurobiological basis of failure to recall extinction memory in posttraumatic stress disorder. Biol. Psychiatr. 66, 1075–1082.

Mork, B.E., Lamerand, S.R., Zhou, S., Taylor, B.K., Sheets, P.L., 2022. Sphingosine-1-phosphate receptor 1 agonist SEW2871 alters membrane properties of late-firing

somatostatin expressing neurons in the central lateral amygdala. Neuropharmacology 203, 108885.
Nishi, D., Hashimoto, K., Noguchi, H., Hamazaki, K., Hamazaki, T., Matsuoka, Y., 2015. Glutamatergic system abnormalities in posttraumatic stress disorder. Psychopharmacology (Berl) 232, 4261–4268.
Ortiz, S., Latsko, M.S., Fouty, J.L., Dutta, S., Adkins, J.M., Jasnow, A.M., 2019. Anterior cingulate cortex and ventral hippocampal inputs to the basolateral amygdala selectively control generalized fear. J. Neurosci. 39, 6526–6539.
Pape, H.C., Pare, D., 2010. Plastic synaptic networks of the amygdala for the acquisition, expression, and extinction of conditioned fear. Physiol. Rev. 90, 419–463.
Ramanathan, K.R., Jin, J., Giustino, T.F., Payne, M.R., Maren, S., 2018. Prefrontal projections to the thalamic nucleus reuniens mediate fear extinction. Nat. Commun. 9, 4527.
Ramirez, K., Shea, D.T., McKim, D.B., Reader, B.F., Sheridan, J.F., 2015. Imipramine attenuates neuroinflammatory signaling and reverses stress-induced social avoidance. Brain Behav. Immun. 46, 212–220.
Ramirez, K., Sheridan, J.F., 2016. Antidepressant imipramine diminishes stress-induced inflammation in the periphery and central nervous system and related anxiety- and depressive- like behaviors. Brain Behav. Immun. 57, 293–303.
Sah, P., Faber, E.S., Lopez De Armentia, M., Power, J., 2003. The amygdaloid complex: anatomy and physiology. Physiol. Rev. 83, 803–834.
Sanacora, G., Treccani, G., Popoli, M., 2012. Towards a glutamate hypothesis of depression: an emerging frontier of neuropsychopharmacology for mood disorders. Neuropharmacology 62, 63–77.
Sanz, E., Yang, L., Su, T., Morris, D.R., McKnight, G.S., Amieux, P.S., 2009. Cell-type-specific isolation of ribosome-associated mRNA from complex tissues. Proc. Natl. Acad. Sci. U. S. A. 106, 13939–13944.
Sawicki, C.M., McKim, D.B., Wohleb, E.S., Jarrett, B.L., Reader, B.F., Norden, D.M., Godbout, J.P., Sheridan, J.F., 2015. Social defeat promotes a reactive endothelium in a brain region-dependent manner with increased expression of key adhesion molecules, selectins and chemokines associated with the recruitment of myeloid cells to the brain. Neuroscience 302, 151–164.
Schwendt, M., Jezova, D., 2000. Gene expression of two glutamate receptor subunits in response to repeated stress exposure in rat hippocampus. Cell. Mol. Neurobiol. 20, 319–329.
Shin, L.M., Liberzon, I., 2010. The neurocircuitry of fear, stress, and anxiety disorders. Neuropsychopharmacology 35, 169–191.
Sierra-Mercado, D., Padilla-Coreano, N., Quirk, G.J., 2011. Dissociable roles of prelimbic and infralimbic cortices, ventral hippocampus, and basolateral amygdala in the expression and extinction of conditioned fear. Neuropsychopharmacology 36, 529–538.
Silveira, M.C., Sandner, G., Graeff, F.G., 1993. Induction of Fos immunoreactivity in the brain by exposure to the elevated plus-maze. Behav. Brain Res. 56, 115–118.
Stuijfzand, S., Creswell, C., Field, A.P., Pearcey, S., Dodd, H., 2018. Research Review: is anxiety associated with negative interpretations of ambiguity in children and adolescents? A systematic review and meta-analysis. JCPP (J. Child Psychol. Psychiatry) 59, 1127–1142.
Sui, L., Wang, Y., Ju, L.H., Chen, M., 2012. Epigenetic regulation of reelin and brain-derived neurotrophic factor genes in long-term potentiation in rat medial prefrontal cortex. Neurobiol. Learn. Mem. 97, 425–440.
Takahashi, A., Chung, J.R., Zhang, S., Zhang, H., Grossman, Y., Aleyasin, H., Flanigan, M. E., Pfau, M.L., Menard, C., Dumitriu, D., Hodes, G.E., McEwen, B.S., Nestler, E.J., Han, M.H., Russo, S.J., 2017. Establishment of a repeated social defeat stress model in female mice. Sci. Rep. 7, 12838.
Teixeira, C.M., Martin, E.D., Sahun, I., Masachs, N., Pujadas, L., Corvelo, A., Bosch, C., Rossi, D., Martinez, A., Maldonado, R., Dierssen, M., Soriano, E., 2011. Overexpression of Reelin prevents the manifestation of behavioral phenotypes related to schizophrenia and bipolar disorder. Neuropsychopharmacology 36, 2395–2405.
Tovote, P., Fadok, J.P., Luthi, A., 2015. Neuronal circuits for fear and anxiety. Nat. Rev. Neurosci. 16, 317–331.
Tropea, T.F., Kosofsky, B.E., Rajadhyaksha, A.M., 2008. Enhanced CREB and DARPP-32 phosphorylation in the nucleus accumbens and CREB, ERK, and GluR1 phosphorylation in the dorsal hippocampus is associated with cocaine-conditioned place preference behavior. J. Neurochem. 106, 1780–1790.
Vertes, R.P., Hoover, W.B., Szigeti-Buck, K., Leranth, C., 2007. Nucleus reuniens of the midline thalamus: link between the medial prefrontal cortex and the hippocampus. Brain Res. Bull. 71, 601–609.
Walf, A.A., Frye, C.A., 2007. The use of the elevated plus maze as an assay of anxiety-related behavior in rodents. Nat. Protoc. 2, 322–328.
Wangler, L.M., Bray, C.E., Packer, J.M., Tapp, Z.M., Davis, A.C., O'Neil, S.M., Baetz, K., Ouvina, M., Witzel, M., Godbout, J.P., 2022. Amplified gliosis and interferon-associated inflammation in the aging brain following diffuse traumatic brain injury. J. Neurosci. 42, 9082–9096.
Wasser, C.R., Herz, J., 2017. Reelin: neurodevelopmental architect and homeostatic regulator of excitatory synapses. J. Biol. Chem. 292, 1330–1338.
Weber, M.D., McKim, D.B., Niraula, A., Witcher, K.G., Yin, W.Y., Sobol, C.G., Wang, Y.F., Sawicki, C.M., Sheridan, J.F., Godbout, J.P., 2019. The influence of microglial elimination and repopulation on stress sensitization induced by repeated social defeat. Biol. Psychiatr. 85, 667–678.
Weger, M., Sandi, C., 2018. High anxiety trait: a vulnerable phenotype for stress-induced depression. Neurosci. Biobehav. Rev. 87, 27–37.
Witcher, K.G., Bray, C.E., Chunchai, T., Zhao, F., O'Neil, S.M., Gordillo, A.J., Campbell, W.A., McKim, D.B., Liu, X., Dziabis, J.E., Quan, N., Eiferman, D.S., Fischer, A.J., Kokiko-Cochran, O.N., Askwith, C., Godbout, J.P., 2021. Traumatic brain injury causes chronic cortical inflammation and neuronal dysfunction mediated by microglia. J. Neurosci. 41, 1597–1616.
Wohleb, E.S., Hanke, M.L., Corona, A.W., Powell, N.D., Stiner, L.M., Bailey, M.T., Nelson, R.J., Godbout, J.P., Sheridan, J.F., 2011. beta-Adrenergic receptor antagonism prevents anxiety-like behavior and microglial reactivity induced by repeated social defeat. J. Neurosci. 31, 6277–6288.
Wohleb, E.S., McKim, D.B., Shea, D.T., Powell, N.D., Tarr, A.J., Sheridan, J.F., Godbout, J.P., 2014a. Re-establishment of anxiety in stress-sensitized mice is caused by monocyte trafficking from the spleen to the brain. Biol. Psychiatr. 75, 970–981.
Wohleb, E.S., Patterson, J.M., Sharma, V., Quan, N., Godbout, J.P., Sheridan, J.F., 2014b. Knockdown of interleukin-1 receptor type-1 on endothelial cells attenuated stress-induced neuroinflammation and prevented anxiety-like behavior. J. Neurosci. 34, 2583–2591.
Wohleb, E.S., Powell, N.D., Godbout, J.P., Sheridan, J.F., 2013. Stress-induced recruitment of bone marrow-derived monocytes to the brain promotes anxiety-like behavior. J. Neurosci. 33, 13820–13833.
Xu, W., Sudhof, T.C., 2013. A neural circuit for memory specificity and generalization. Science 339, 1290–1295.
Yin, W., Gallagher, N.R., Sawicki, C.M., McKim, D.B., Godbout, J.P., Sheridan, J.F., 2019. Repeated social defeat in female mice induces anxiety-like behavior associated with enhanced myelopoiesis and increased monocyte accumulation in the brain. Brain Behav. Immun. 78, 131–142.
Yin, W., Swanson, S.P., Biltz, R.G., Goodman, E.J., Gallagher, N.R., Sheridan, J.F., Godbout, J.P., 2022. Unique brain endothelial profiles activated by social stress promote cell adhesion, prostaglandin E2 signaling, hypothalamic-pituitary-adrenal axis modulation, and anxiety. Neuropsychopharmacology.
Zelikowsky, M., Bissiere, S., Hast, T.A., Bennett, R.Z., Abdipranoto, A., Vissel, B., Fanselow, M.S., 2013. Prefrontal microcircuit underlies contextual learning after hippocampal loss. Proc. Natl. Acad. Sci. U. S. A. 110, 9938–9943.
Zelikowsky, M., Hersman, S., Chawla, M.K., Barnes, C.A., Fanselow, M.S., 2014. Neuronal ensembles in amygdala, hippocampus, and prefrontal cortex track differential components of contextual fear. J. Neurosci. 34, 8462–8466.
Zhao, T., Gao, X., Huang, G.B., 2021. Effects of chronic social defeat stress on behavior and dopamine receptors in adolescent mice with 6-hydroxydopamine lesions of the medial prefrontal cortex. Front. Behav. Neurosci. 15, 731373.